

<https://doi.org/10.1038/s42003-025-07981-5>

Isolation and cultivation of a novel freshwater magnetotactic coccus FCR-1 containing unchained magnetosomes



Hirokazu Shimoshige^{1,2}✉, Keiichi Yanagisawa¹, Masayuki Miyazaki², Yoshihiro Takaki², Shigeru Shimamura², Hidetaka Nomaki², Mizuki Fukui³, Hiroki Shirakawa³, Hideki Kobayashi¹, Azuma Taoka^{3,4} & Toru Maekawa^{1,5}

Magnetotactic bacteria are ubiquitous aquatic prokaryotes that have the ability to biomineralize magnetite (Fe₃O₄) and/or greigite (Fe₃S₄) nanoparticles called magnetosomes. Magnetotactic cocci belonging to the class “Ca. Magnetococcia” are most frequently identified in freshwater habitats, but remain uncultivated. Here, we report for the first time axenic cultivation of freshwater magnetotactic coccus FCR-1 isolated from Chichijima, Japan. Strain FCR-1 grows microaerophilically in a semi-solid gellan gum medium. We find that strain FCR-1 biomineralizes Fe₃O₄ nanoparticles, which are not chained, into a cell. Based on phylogenomic analysis, compared with strains of the class “Ca. Magnetococcia”, strain FCR-1 represents a novel genus of candidate family “Ca. Magnetaquicoccaceae” within the class “Ca. Magnetococcia” and we tentatively name this novel genus “Ca. Magnetaquiglobus chichijimensis”. Our isolate provides a promising tool for elucidating the functions of unchained magnetosomes, the global distribution of magnetotactic bacteria and the origin of magnetotaxis.

Chichijima; one of the Ogasawara (Bonin) Islands, which are volcanic islands formed during the Eocene time between 46 and 48 Ma, is located in the northwestern region of the Pacific Ocean, approximately 1000 km south from the Japanese mainland¹. The Oceanic islands, which are remote and isolated from the continental landmass, have been considered a suitable model for evolutionary studies². Because the Bonin Islands have never been connected to any continental landmass, quite a few endemic terrestrial species have been found in the islands^{3–5}. Thus, it is still believed that the Bonin Islands could provide a clue to a better understanding of the distribution and evolution of organisms on earth.

Magnetotactic bacteria (MTB) are phylogenetically a diverse group of prokaryotes that biomineralize intracellular magnetosomes, which are proteolipid membrane-enclosed magnetic nanoparticles (NPs) composed of magnetite (Fe₃O₄) and/or greigite (Fe₃S₄). Magnetosomes are generally characterized by a distinct species-specific crystal morphology and the arrangement in chains within the cells^{6,7}. Thanks to the linear arrangement of magnetosomes, MTB have the ability to swim along geomagnetic field lines, a behaviour known as magnetotaxis⁶. MTB are microaerophiles or

anaerobes that mainly inhabit the oxic-anoxic transition zones (OATZs) in the sediment or chemically stratified water column⁸.

To our knowledge, known MTB species are affiliated with the classes *Alphaproteobacteria*, *Gammaproteobacteria*, *Zetaproteobacteria*, “Ca. Magnetococcia” of the phylum *Pseudomonadota*, and with the phyla SAR324, *Desulfobacterota*, *Bdellovibrionota*, *Nitrospirota*, *Nitrospinota*, *Fibrobacterota*, *Omniotrophota*, *Latescibacterota*, *Planctomycetota*, *Riflobacterota*, *Hydrogenedentota*, UBA10199 and *Elusimicrobiota* in the GTDB taxonomy^{9–12}. Magnetotactic cocci belonging to the class “Ca. Magnetococcia” are most commonly observed morphotype among MTB and frequently detected from both freshwater and marine habitats¹³. However, only five magnetotactic cocci from marine habitats and hypersaline lagoon have been isolated in axenic cultures; i.e., *Magnetococcus marinus* MC-1^{14,15}, “Ca. Magnetococcus massalia” MO-1¹⁶, *Magnetofaba australis* IT-1¹⁷, and strain PR-3 and SS-1¹⁸.

Besides the biomineralization of iron oxide crystals, it is known that magnetotactic cocci possess intracellular polyphosphate (Poly P) granules that frequently occupy most of the cell volume, whereas those also possess

¹Bio-Nano Electronics Research Centre, Toyo University, 2100 Kujirai, Kawagoe, Saitama, 350-8585, Japan. ²Institute for Extra-cutting-edge Science and Technology Avant-garde Research (X-star), Japan Agency for Marine-Earth Science and Technology (JAMSTEC), 2-15 Natsushima-cho, Yokosuka, Kanagawa, 237-0061, Japan. ³Institute of Science and Engineering, Kanazawa University, Kakuma-machi, Kanazawa, Ishikawa, 920-1192, Japan. ⁴Nano Life Science Institute (WPI-NanoLSI), Kanazawa University, Kakuma-machi, Kanazawa, Ishikawa, 920-1192, Japan. ⁵Graduate School of Interdisciplinary New Science, Toyo University, 2100 Kujirai, Kawagoe, Saitama, 350-8585, Japan. ✉e-mail: shimoshige552@toyo.jp

intracellular sulphur granules, which indicates the capability of utilizing reduced sulphur compounds¹⁹. The capability of forming the Poly P granules indicates that magnetotactic cocci utilize a large amount of phosphorus for supporting the “bacterial shuttle” around OATZ^{20–22}. Three cultured strains; *Mc. marinus* MC-1¹⁵, “*Ca. Mc. massalia*” MO-1¹⁶ and *Mf. australis* IT-1¹⁷, which are microaerophiles, utilize thiosulphate for autotrophic growth. The metagenomic analysis indicated that uncultured freshwater magnetotactic coccus “*Ca. Magnetaquicoccus inordinatus*” UR-1 was potentially capable of oxidizing sulphide, while it also appeared to have a potential to oxidize sulphite produced in dissimilatory sulphur oxidation¹⁹. Therefore, it is supposed that magnetotactic cocci play an important role in a biogeochemical cycling of iron, phosphorus and sulphur in natural environments^{23,24}.

Due to the difficulty of isolating freshwater magnetotactic cocci in an axenic culture, the diversity and microbial ecology of cocci and the characterization of magnetosomes biomineralized by cocci have been mainly investigated by cultivation-independent methods using fluorescent in situ hybridization (FISH) with specific 16S rRNA-based probes and FISH coupled with transmission electron microscopy (FISH-TEM) and scanning electron microscopy (FISH-SEM). These approaches have revealed that freshwater magnetotactic cocci are highly diverse in terms of the size, number, morphology and arrangement of magnetosome crystals^{13,19,25}. Especially, the spatial arrangement of magnetosome crystals within the cells varies among strains of uncultured freshwater magnetotactic cocci. Strain YQC-1, BHC-1, DMHC-1, WYHC-1 and WYHC-3 biomineralize a single chain of magnetosome in each cell, while strain MYC-4, MYC-5, YQC-3, YQC-5 and XQGC-1 double chains of magnetosomes within a cell. Strain DMHC-2, DMHC-8 and MYC-9 biomineralize two double chains of magnetosomes in a cell, whereas “*Ca. Mq. inordinatus*” UR-1, strain WYHC-2, THC-1, MYC-3, MYC-7, DMHC-6 and YQC-9 unchained magnetosomes^{13,19,25,26}. Intriguingly, unchained magnetosomes have been frequently found in magnetotactic cocci from freshwater habitats^{13,19,25}. Now, a question; “How can the cocci sense the geomagnetic field lines with unchained magnetosomes” arises. Freshwater magnetotactic cocci biomineralizing unchained magnetosomes have not yet been cultivated. The cultivation and isolation of these magnetotactic cocci are essential to understand the diversity and ecological functions of cocci in freshwater habitats and elucidate the functions and evolution of unchained magnetosomes.

In this study, we for the first time cultivate novel magnetotactic coccus FCR-1 isolated from Renju Dam in Chichijima and investigate the characteristics of strain FCR-1. Magnetotactic coccus FCR-1 is cultivated using a semi-solid medium using gellan gum as a gelling agent. We find that the spatial arrangement and morphology of magnetosome crystals of strain FCR-1 are different from those of three cultured *Mc. marinus* MC-1, “*Ca. Mc. massalia*” MO-1 and *Mf. australis* IT-1. We also conduct the whole genome sequencing to obtain functional annotations of genes related to the formation of the magnetosome. We also find, comparing the genome of strain FCR-1 with the available “*Ca. Magnetococcia*” genomes, that strain FCR-1 represents a novel genus of candidate family “*Ca. Magnetaquicoccaceae*” within the class “*Ca. Magnetococcia*”, tentatively named “*Ca. Magnetaquiglobus chichijimensis*”.

Results

Isolation and phylogenetic analysis of strain FCR-1

After five-month incubation of the freshwater and sediment sample, MTB cells were grown in a microcosm (Fig. 1a, b). The pH of water in the microcosm was 8.3, the salinity was less than 1 ppt and the chemical oxygen demand (COD) was 16.0 mg L⁻¹. We observed that the MTB lived in the surface layer between -2 and -1 cm of sediment, noting that the OATZ ranged from -1 to 0.5 cm (Fig. 1c, d and Supplementary Data). In the present case, magnetotactic cocci were the most dominant MTB, whereas neither spirillum, vibrio nor rod-shaped MTB were detected (Fig. 1c). The concentrations of NO₃⁻ drastically decreased in the surface layer between -2 and -1 cm of sediment, where magnetotactic coccus cells were

observed, whereas the concentrations of NH₄⁺ slightly increased in the same layer of sediment. The microbial communities based on V3-V4 16S rRNA regions after magnetic enrichment of MTB using the MTB trap device²⁷ consisted of *Magnetococcales* (50.1%), *Eubacteriales* (18.4%), *Pseudomonadales* (11.4%), *Chlorellales* (5.0%), *Lactobacillales* (4.8%), *Propionibacteriales* (4.7%), *Burkholderiales* (2.8%) and *Hyphomicrobiales* (2.6%) at the order level (Fig. 1d and Supplementary Data). The most dominant order was *Magnetococcales*, which corresponded to magnetotactic cocci detected from the surface layer of sediment of the microcosm (Supplementary Fig. 1 in the Supplementary Information).

We successfully cultivated freshwater magnetotactic coccus FCR-1 at room temperature in dim light for 14 days using the Freshwater magnetotactic cocci (FMC) medium, which was designed based on the physicochemical parameters (e.g., NO₃⁻, NH₄⁺ and dissolved oxygen (DO) concentrations) and distribution of MTB in the microcosm. We confirmed the establishment of the axenic culture by an optical microscope and TEM, and the direct sequencing of 16S rRNA gene PCR products without cloning. The 16S rRNA gene sequence analysis showed that strain FCR-1 (1,423 bp) was affiliated with the class “*Ca. Magnetococcia*” (Fig. 2). The 16S rRNA gene sequence of strain FCR-1 was the same as that of the uncultured magnetotactic coccus clone HCH0515 (accession number: JX134734) (100%) from freshwater sediments of moat, Xi'an city, China²⁸ and closely related to the cultured *Mf. australis* IT-1 (accession number: JX534168) (89.7%)¹⁷, *Mc. marinus* MC-1 (accession number: NR_074371) (89.2%)¹⁵ and “*Ca. Mc. massalia*” MO-1 (accession number: EF643520) (88.7%)¹⁶. The 16S rRNA gene sequence was 94.1% similar to the sequence of uncultured magnetotactic coccus “*Ca. Mq. inordinatus*” UR-1 (accession number: MK813936) collected from a freshwater habitat of Uda River, Ulan-Ude, Eastern Siberia, Russia¹⁹, which biomineralizes unchained magnetosomes.

Growth, morphology and structure of FCR-1 cells

To investigate the optimal conditions for growth, strain FCR-1 was grown heterotrophically in the FMC medium supplemented with 10 mM HEPES buffer (pH7.8) (except for optimum pH tests) under various growth conditions in dim light for 14 days (Supplementary Figs. 2, 3 in the Supplementary Information). The growth of strain FCR-1 was confirmed by the formation of a white-coloured band of cells at the OATZ (pink-colourless interface). Strain FCR-1 grew in the presence of 0.7–3.9% O₂, while the cells were unable to grow anaerobically. Although strain FCR-1 was able to grow at 20–32 °C, it grew fastest at a temperature range of 24–28 °C. The formation of a very fine band of cells was observed when grown at 20 °C. The optimal pH for the growth of strain FCR-1 was 7.8 although it was able to grow at pH7.4–8.2 with HEPES buffer. A band of cells was not observed when grown at pH8.2 with Bicine buffer. Strain FCR-1 grew in the presence of 0–25 μM ferrous chloride without any differences in the growth rate. Strain FCR-1 grew in the semi-solid medium containing 1.5–6.0 g L⁻¹ of gellan gum. Strain FCR-1 was also able to grow in the semi-solid medium using Bacto agar as a gelling agent, whereas the cells were unable to grow in the medium using Noble agar. Strain FCR-1 used only acetate among examined substrates as a carbon and/or energy source for supporting the heterotrophic growth (Table 1 and Supplementary Fig. 3 in the Supplementary Information). The formation of a band of cells was not observed when grown in the casamino acids- and acetate-free FMC medium containing sodium bicarbonate as a major carbon source and thiosulphate or sulphite as an electron donor, whereas the growth was observed when grown in the presence of sulphide as an electron donor. Therefore, strain FCR-1 had the ability to grow chemolithoautotrophically using sulphide as an electron donor, but it grew slowly and formed a fine band of cells at the OATZ after 21 days of inoculation. Strain FCR-1 was unable to use sulphate or sulphite as an electron acceptor for dissimilatory sulphate reduction.

Strain FCR-1 grew well under heterotrophic conditions using the FMC medium supplemented with 10 mM HEPES buffer (pH7.8) at room temperature in dim light in the presence of approximately 0.7% O₂ and formed a band of cells at the OATZ (Fig. 3a). Strain FCR-1 formed a fine band of cells

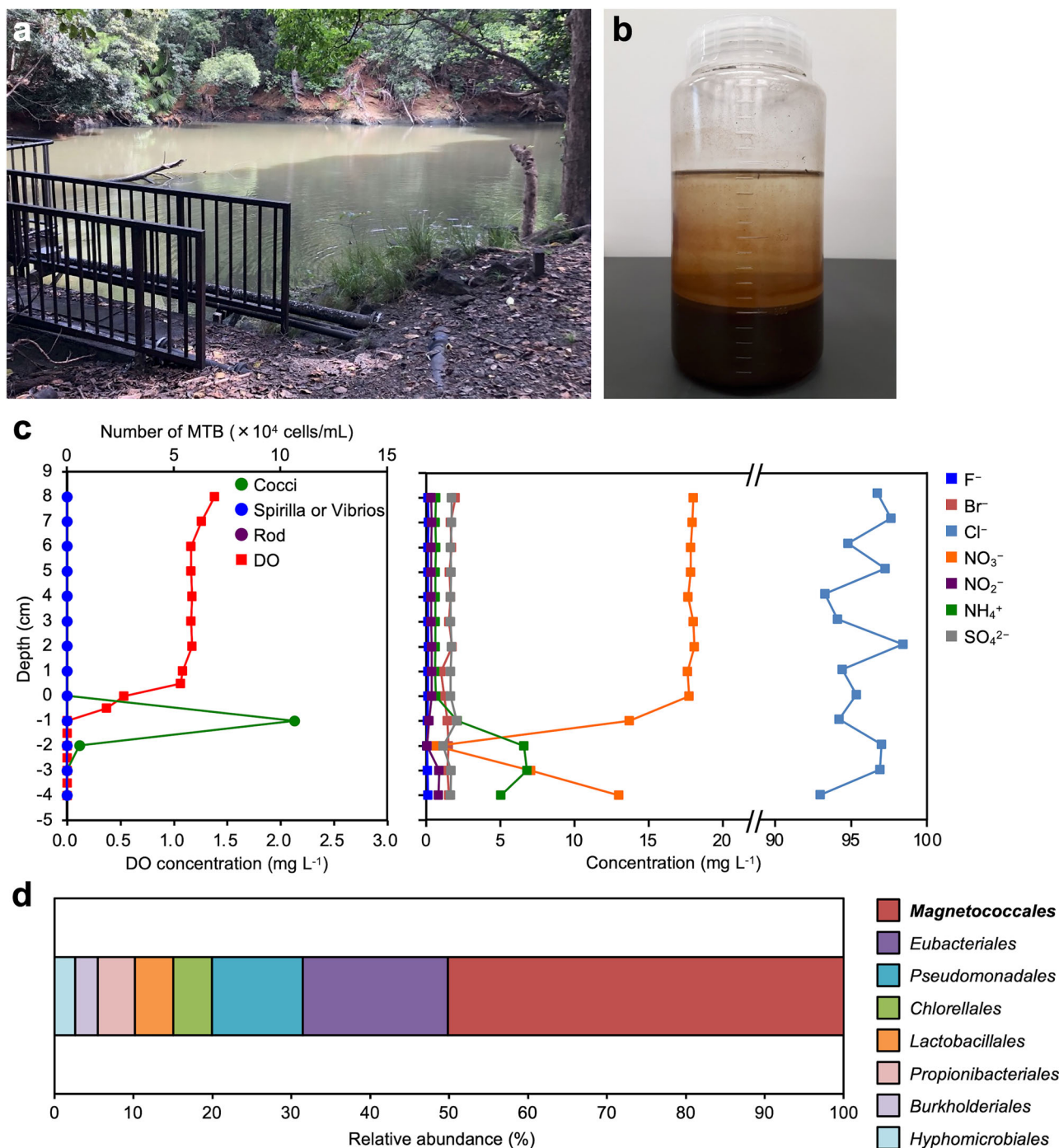


Fig. 1 | Overview of the sampling site and the distribution of MTB and chemical species in a microcosm. **a** Overview of the sampling site of Renju Dam located in Chichijima. **b** Plastic bottle containing freshwater and sediment samples collected from Renju Dam. **c** Vertical distribution of MTB and DO concentration (left graph), and the vertical distribution of fluoride (F^-), bromide (Br^-), chloride (Cl^-), nitrate

(NO_3^-), nitrite (NO_2^-), ammonium (NH_4^+), sulphate (SO_4^{2-}) and phosphate (PO_4^{3-}) concentrations (right graph) in a microcosm. Phosphate ions were undetectable ($<0.3 \text{ mg L}^{-1}$). **d** Composition of the microbial communities magnetically enriched from the microcosm.

after 24 h of incubation. The band of cells moved upwards with an increase of the incubation time. After 7 days of incubation, the band of cells became thicker presumably using oxygen present in the headspace of the tube. Furthermore, strain FCR-1 formed a broad band of cells just below the surface of the medium after 14 days of incubation. The oxygen (O_2) concentration around the band of cells was measured over 14 days (Supplementary Fig. 4 in the Supplementary Information). After 7 days of incubation, the band of cells was positioned between 0 and $13.2 \mu\text{M } O_2$ (Supplementary Fig. 4a in the Supplementary Information). Strain FCR-1

consumed most of oxygen as an electron acceptor after 14 days of incubation (Supplementary Fig. 4b in the Supplementary Information).

The morphology of strain FCR-1 was either coccoid or ovoid, the length and width of which were $1.7 \pm 0.2 \mu\text{m}$ and $1.4 \pm 0.1 \mu\text{m}$ ($n = 100$). Strain FCR-1 responded to a magnetic field generated by a bar magnet (80 mT) and exhibited North-seeking polar magnetotaxis under oxic conditions confirmed by the hanging drop method (Fig. 3b). Strain FCR-1 swam at a speed of $58.2 \pm 9.8 \mu\text{m/s}$ ($n = 343$) in the FMC medium under the microaerobic condition ($0.1\% O_2$) and a helical trajectory was observed

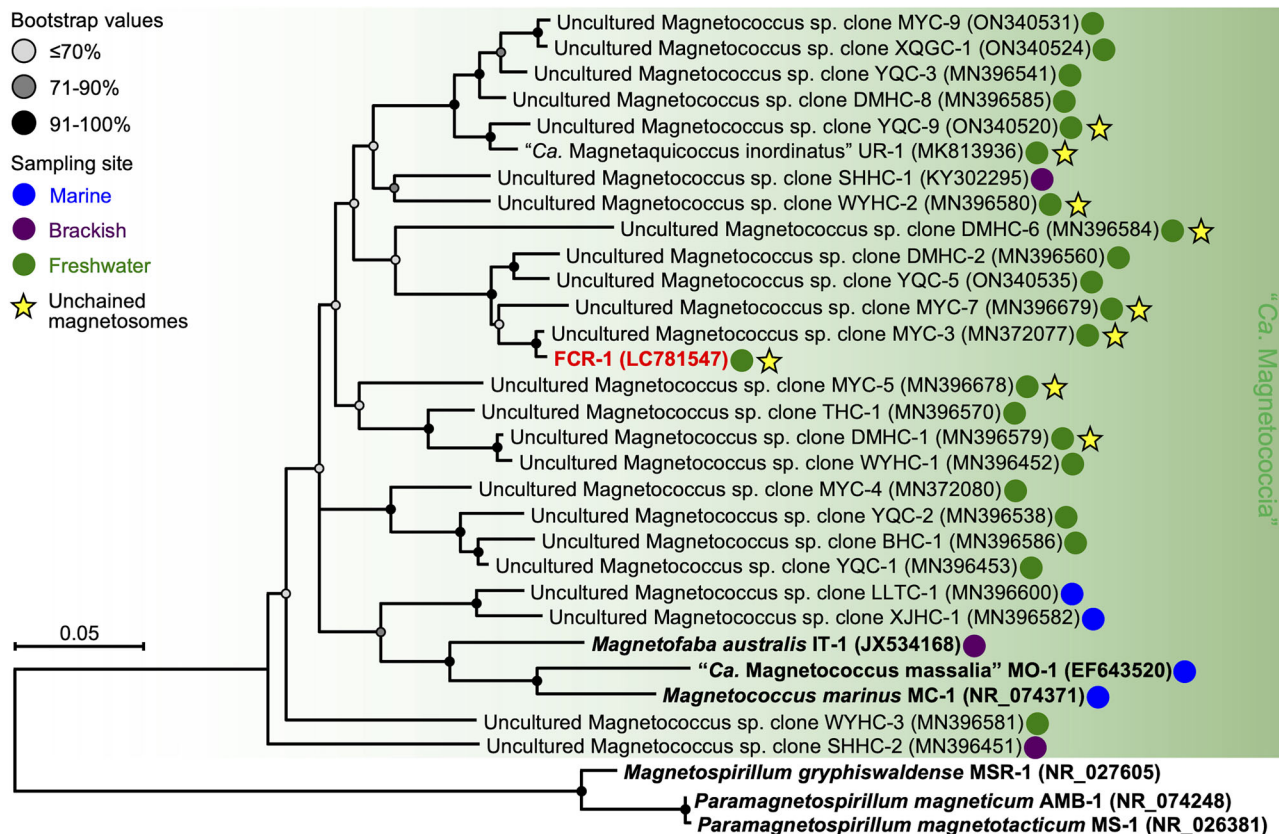


Fig. 2 | Phylogenetic tree based on 16S rRNA gene sequences. A maximum-likelihood (ML) tree based on 16S rRNA gene sequences showing the position of strain FCR-1 and 28 uncultured and cultured strains of magnetotactic "Ca. Magnetococcia". Bootstrap values at the nodes are shown as percentages of 1000 replicates. The 16S rRNA gene sequences of the magnetotactic *Alphaproteobacteria*, *Magnetospirillum gryphiswaldense* MSR-1, *Paramagnetospirillum magneticum*

MS-1 and *Paramagnetospirillum magneticum* AMB-1 are used as the outgroup. GeneBank accession numbers are given in parentheses. Circle symbols indicate the sampling sites of the magnetotactic cocci; marine (blue circles), brackish (purple circles) and freshwater habitats (green circles). Star symbols indicate the magnetotactic cocci biomineralizing unchained magnetosomes. Cultured MTB are shown in bold. The scale bar represents nucleotide substitution per site.

by bright-field optical microscopy (Fig. 3c). Strain FCR-1 biomineralized unchained magnetosomes (Fig. 3d). The number of magnetic NPs per cell was 14 ± 4 ($n = 100$). When the cells were grown chemolithoautotrophically using sulphide as an electron donor, the number of magnetic NPs per cell was 21 ± 9 ($n = 100$). Almost all of the cells biomineralized unchained magnetosomes (96%, $n = 100$), while the other cells biomineralized magnetosomes arranging chain structures (4%, $n = 100$) (Supplementary Fig. 5 in the Supplementary Information). Strain FCR-1 possessed two bundles of flagella on one side of each cell (bilophotrichous) (Fig. 3d). The two bundles of flagella were composed of fifteen individual filaments (Fig. 3e). The diameter of a flagellum was 10.5 ± 0.8 nm ($n = 277$). The number of flagellar filaments in strain FCR-1 was unequivocally different from that of flagellar filaments in three cultured *Mc. marinus* MC-1¹⁵, "Ca. Mc. massalia" MO-1¹⁶ and *Mf. australis* IT-1¹⁷ (Table 1). Besides biomineralizing the magnetosomes composed of iron and oxygen, strain FCR-1 also had the capability of forming Poly P granules into the cell (Fig. 3f, g and Supplementary Figs. 6, 7 in the Supplementary Information), noting that 1–3 Poly P granules were formed in each cell and almost all of the cells possessed 2 Poly P granules (96%, $n = 100$) when grown in the semi-solid gellan gum medium for 14 days. Additionally, the Poly P granules contained alkaline earth metals (Mg, Ca) and alkali metals (Na, K), and a relatively large amount of either magnesium (Mg Ka/P Ka = 0.34 ± 0.02 , Ca Ka/P Ka = 0.01 ± 0.01) or calcium (Mg Ka/P Ka = 0.12 ± 0.02 , Ca Ka/P Ka = 0.28 ± 0.02) were detected in the granules in individual cells (Fig. 3f, g, Supplementary Figs. 6, 7 in the Supplementary Information and Supplementary Data). Most of the cells formed the Poly P granules containing magnesium (75%, $n = 100$), whereas the other cells formed the Poly P granules containing calcium (25%, $n = 100$). In addition, strain FCR-1 formed a sulphur granule in the cell

when grown chemolithoautotrophically using sulphide as an electron donor (Supplementary Fig. 8 in the Supplementary Information).

Characterization of magnetosomes in strain FCR-1

HRTEM images of magnetosomes revealed that the magnetic NPs were truncated hexagonal prismatic crystals composed of iron oxide (Fig. 4a and Supplementary Fig. 9c in the Supplementary Information). The EELS spectrum of the iron oxide NPs showed that the Fe-L₂ and Fe-L₃ edges were, respectively, located at 709.2 and 722.5 eV, which corresponded to the spectrum of Fe₃O₄ rather than that of Fe₂O₃ (Fig. 4b, Supplementary Fig. 9b in the Supplementary Information and Supplementary Data). The HRTEM images of the truncated hexagonal prismatic Fe₃O₄ NPs showed that the side faces of the prisms were {220} faces, whereas the bottom and top ones {111} faces and truncated ones {111} faces (Fig. 4c and Supplementary Figs. 9, 10 in the Supplementary Information). The twin crystals of the truncated hexagonal prismatic Fe₃O₄ NPs were also occasionally observed in the FCR-1 cell (Supplementary Fig. 10d in the Supplementary Information). The length (long axis) of the truncated hexagonal prismatic Fe₃O₄ NPs was 77.1 ± 13.7 nm, while the width (perpendicular to the long axis) of the Fe₃O₄ NPs was 50.4 ± 9.7 nm, when grown heterotrophically ($n = 507$) (Fig. 4d, e and Supplementary Data). The shape factor (width divided by length) of the truncated hexagonal prismatic Fe₃O₄ NPs was 0.65 ± 0.08 ($n = 507$) (Fig. 4f and Supplementary Data).

Phylogenetic analysis based on whole-genome sequence

The obtained genome sequence consisted of 5 contigs, with a total length of 4,187,411 bp. The genome completeness and contamination were 99.7% and 0.5%, respectively. The GC content of the genome sequence was

Table 1 | Comparison of the characteristics of strain FCR-1 with those of cultured *Magnetofaba australis* IT-1, “*Ca. Magnetococcus massalia*” MO-1 and *Magnetococcus marinus* MC-1

Characteristics	FCR-1	<i>Magnetofaba australis</i> IT-1 ^a	“ <i>Ca. Magnetococcus massalia</i> ” MO-1 ^b	<i>Magnetococcus marinus</i> MC-1 ^c
Isolation source	Renju Dam, Chichijima Island, Japan (Freshwater environment)	Itaipu Lagoon, Rio de Janeiro, Brazil (Brackish to Marine environment)	Mediterranean Sea, Pointe Rouge, France (Marine environment)	Pettaquamscutt Estuary, Rhode Island, America (Marine environment)
Cell morphology	Coccoid or ovoid	Coccoid or ovoid	Ovoid	Coccoid
Number of flagella	2 bundles of 15 flagella	2 bundles of 7 flagella	2 bundles of 7 flagella	2 bundles of 7 flagella
Arrangement of magnetosome	Unchain structure	Chain structure	Chain structure	Chain structure
Morphology of magnetosome	Putative truncated hexagonal prismatic crystal	Elongated octahedral crystal	Elongated cubo-octahedral crystal	Elongated hexagonal prismatic crystal
Number of magnetosome per cell	14 ± 4 (heterotrophic) 21 ± 9 (autotrophic)	10 ± 3 (heterotrophic) 6 ± 4 (autotrophic)	17 ± 5 (autotrophic)	14 ± 3 (heterotrophic) 10 ± 2 (autotrophic)
Length of magnetosome (nm)	77 ± 14 (heterotrophic)	83 ± 26 (heterotrophic)	64 ± 20 (autotrophic)	83 ± 14 (heterotrophic) 72 ± 11 (autotrophic)
Width of magnetosome (nm)	50 ± 10 (heterotrophic)	74 ± 23 (heterotrophic)	57 ± 17 (autotrophic)	78 ± 11 (heterotrophic) 70 ± 13 (autotrophic)
Shape factor (width/length) of magnetosome	0.65 ± 0.08 (heterotrophic)	0.89 ± 0.05 (heterotrophic)	0.89 (autotrophic)	0.94 (heterotrophic) 0.97 (autotrophic)
Electron donor (with oxygen as an electron acceptor):				
Thiosulphate	–	+	+	+
Sulphide	+	ND	–	+
Potential carbon source (to support heterotrophic growth):				
Acetate	+	+	ND	+
Succinate	–	+	ND	–

Values represent mean ± standard deviation (SD).
+ Positive reaction, – negative reaction, ND not determined.
^a Morillo et al.¹⁷
^b Lefèvre et al.¹⁸
^c Bazylinski et al.¹⁵

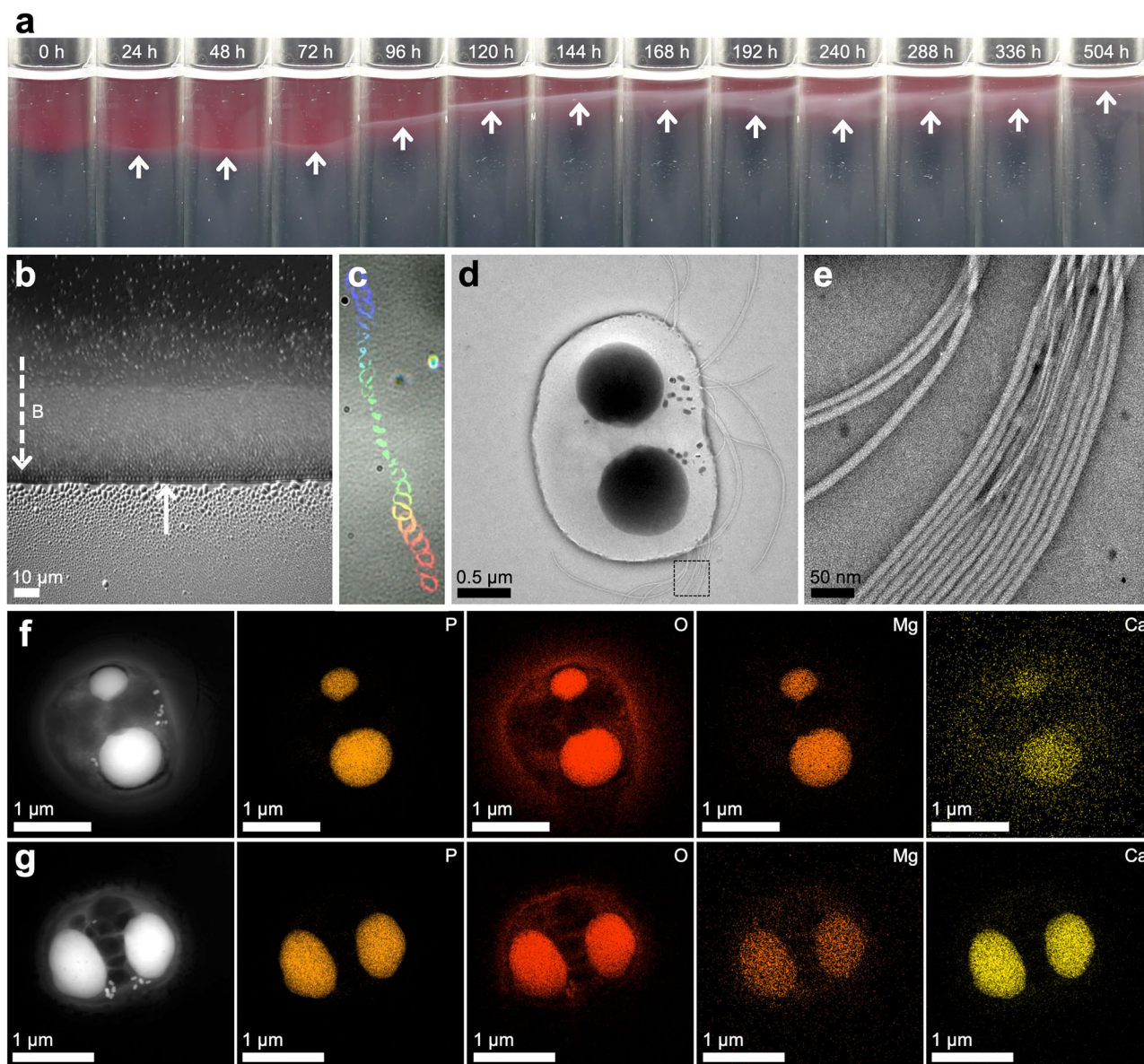


Fig. 3 | Characterization of FCR-1 cells grown in a semi-solid gellan gum medium containing oxygen concentration gradients. **a** Growth of FCR-1 cells in the modified FMC medium at room temperature in dim light over 3 weeks. The growth occurs as a band of cells in the oxic-anoxic transition zone (OATZ). The band of cells is indicated by a white arrow. **b** Differential interference contrast (DIC) image of FCR-1 cells swimming along the applied magnetic field B indicated by a white dotted arrow. FCR-1 cells were accumulated at the edge of droplets (indicated by a white arrow). **c** Swimming trajectory of an FCR-1 cell along the applied magnetic field. **d** TEM image of a negatively stained (0.25% phosphotungstic acid) FCR-1 cell with

coccoid or ovoid morphology, two flagella bundles on one side of the cell and unchained magnetosomes. **e** Close-up TEM image of the area outlined in the black dashed rectangle in **c**. The TEM image exhibits fifteen flagellar filaments of the FCR-1 cell. **f** STEM-EDS elemental maps of an FCR-1 cell forming Poly P granules containing magnesium. STEM-ADF images of the cell, and corresponding elemental maps of P (P K α), O (O K α), Mg (Mg K α) and Ca (Ca K α). **g** STEM-EDS elemental maps of an FCR-1 cell forming Poly P granules containing calcium. STEM-ADF images of an FCR-1 cell, and corresponding elemental maps of P (P K α), O (O K α), Mg (Mg K α) and Ca (Ca K α).

61.4 mol%. The genome possessed one *rrn* operon of 5S rRNA (locus_tag: SIID45300_00398), 16S rRNA gene (locus_tag: SIID45300_00396) and 23S rRNA gene (locus_tag: SIID45300_00397). The 16S rRNA gene of the genome sequence was identical to that (accession number: LC781547) obtained from the direct sequencing method.

The phylogenomic tree based on ubiquitous single-copy marker genes showed that strain FCR-1 formed a clade together with uncultured *Magnetococcus* sp. YQC-9, uncultured *Magnetococcus* sp. YQC-5, “*Ca. Mq. inordinatus*” UR-1, uncultured *Magnetococcus* sp. MYC-9, uncultured *Magnetococcus* sp. DMHC-8, uncultured *Magnetococcus* sp. XQGC-1 and uncultured *Magnetococcus* sp. YQC-3, while *Mf. australis* IT-1, “*Ca. Mc. massalia*” MO-1 and *Mc. marinus* MC-1 formed a separate clade (Fig. 5a). The average amino acid identity (AAI) analysis is usually used for taxon

separation at the family and genus levels using numerical indices based on the amino acid sequences of the genome. The AAI analysis of strain FCR-1 showed the identity values ranging from 49.1 to 98.1% between strains of the class “*Ca. Magnetococcia*” (Fig. 5b). The previous study has demonstrated that the AAI values of 55–56% were correlated with the separating families within the class “*Ca. Magnetococcia*”, while those of 64–65% were applied for the separation of genera¹⁹. The AAI values of strain FCR-1 were, respectively, 79.6%, 63.5%, 56.6%, 57.0%, 57.6%, 56.9% and 55.4% with strain YQC-9 and YQC-5, “*Ca. Mq. inordinatus*” UR-1 and strain MYC-9, DMHC-8, XQGC-1 and YQC-3. The AAI analysis also showed the identity values were 55.0%, 54.1%, 54.5%, 52.1%, 52.4%, 51.4% and 51.7% with strain DMHC-6, DMHC-1, THC-1, WYHC-3, *Mf. australis* IT-1, “*Ca. Mc. massalia*” MO-1 and *Mc. marinus* MC-1. Therefore, strain FCR-1 was

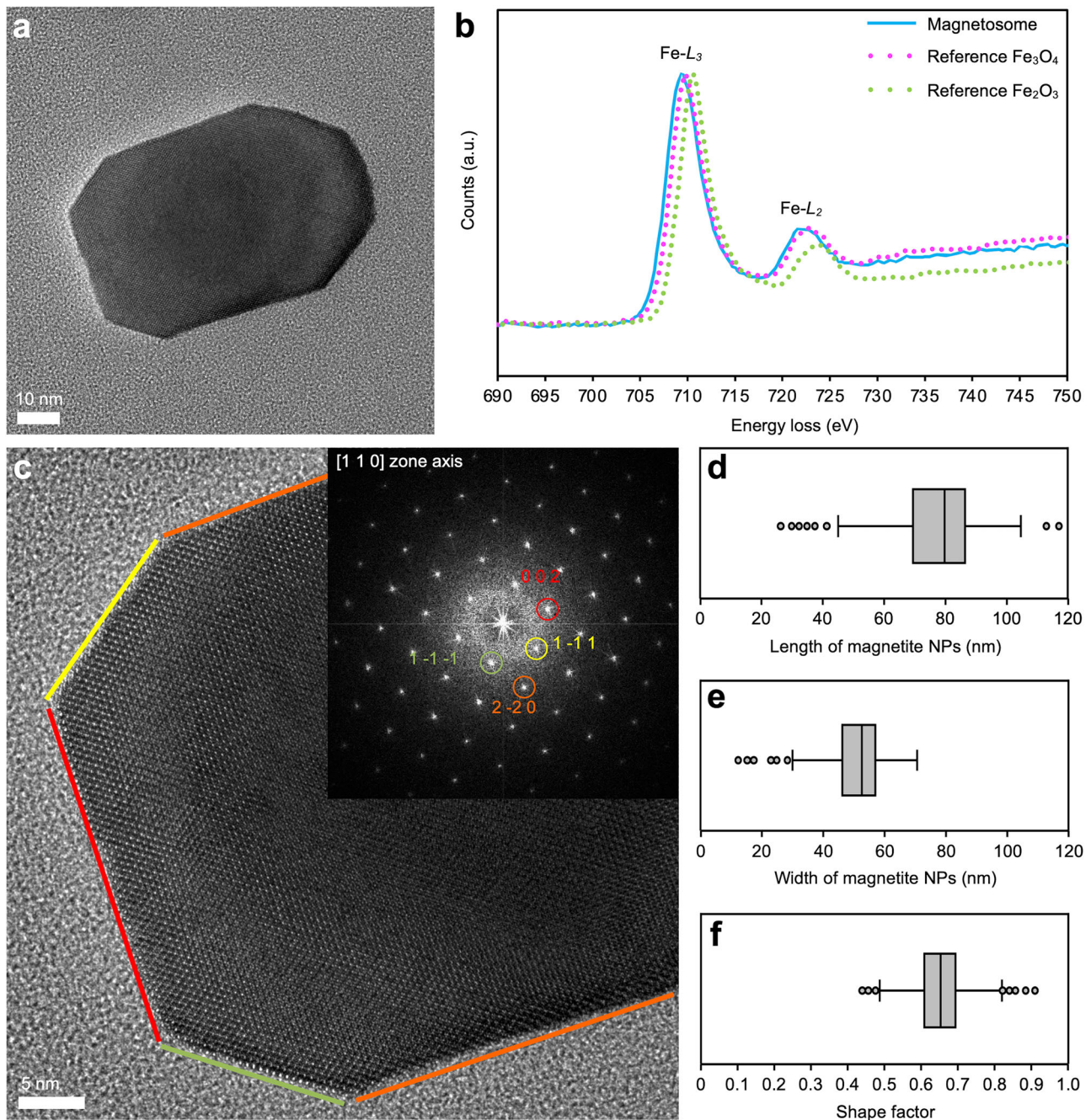


Fig. 4 | Characterization of magnetosomes in strain FCR-1. **a** HRTEM image of an iron oxide NP in an FCR-1 cell. **b** EELS spectrum measured at Fe $L_{2,3}$ edges of the iron oxide NP. The spectrum is compared with the spectra of reference Fe_3O_4 and Fe_2O_3 . **c** HRTEM analysis of the Fe_3O_4 NP obtained along the $[110]$ zone axis and the fast Fourier transform (FFT) pattern. (002), (1-1-1), (1-11) and (2-20) crystal faces are indicated by red, green, yellow and orange solid circles, respectively. Box plots of

length (**d**), width (**e**) and shape factor (**f**) of Fe_3O_4 NPs in FCR-1 cells grown under heterotrophic conditions. The length, width and shape factor of each box represented the central range covering 50% of the distribution, the horizontal line represented median and the bar ends corresponded to the maximum and minimum values of each distribution.

affiliated with the family “*Ca. Magnetaquicoccaceae*” and represented the distinct genus of “*Ca. Mq. inordinatus*” UR-1 and strain YQC-5, MYC-9, DMHC-8, XQGC-1 and YQC-3. Strain DMHC-6, DMHC-1, THC-1 and WYHC-1 were classified into separate families. The genome sequence-based indexes average nucleotide identity (ANI) and digital DNA-DNA hybridization (dddH) are generally used for taxonomic classification at the species levels. The ANI analysis of strain FCR-1 showed the identity values ranging from 70.1 to 100% between strains of the class “*Ca. Magnetococcia*” (Supplementary Fig. 11a in the Supplementary Information), noting that it is well known that when the ANI values are below 95%, the samples are

counted as distinct species²⁹. The dddH analysis of strain FCR-1 showed the identity values ranging from 15.2 to 97.5% (Supplementary Fig. 11b in the Supplementary Information). The dddH values were also below the standard species separation threshold (<70%)³⁰, indicating that strain FCR-1 represented distinct species of strain YQC-9.

Magnetosome- and magnetotaxis-associated genes

Thanks to a nearly complete genome obtained from strain FCR-1, a magnetosome gene cluster (MGC) (48,074 bp) was identified. Two genes encoding putative transposase (locus_tag: SIID45300_02188,

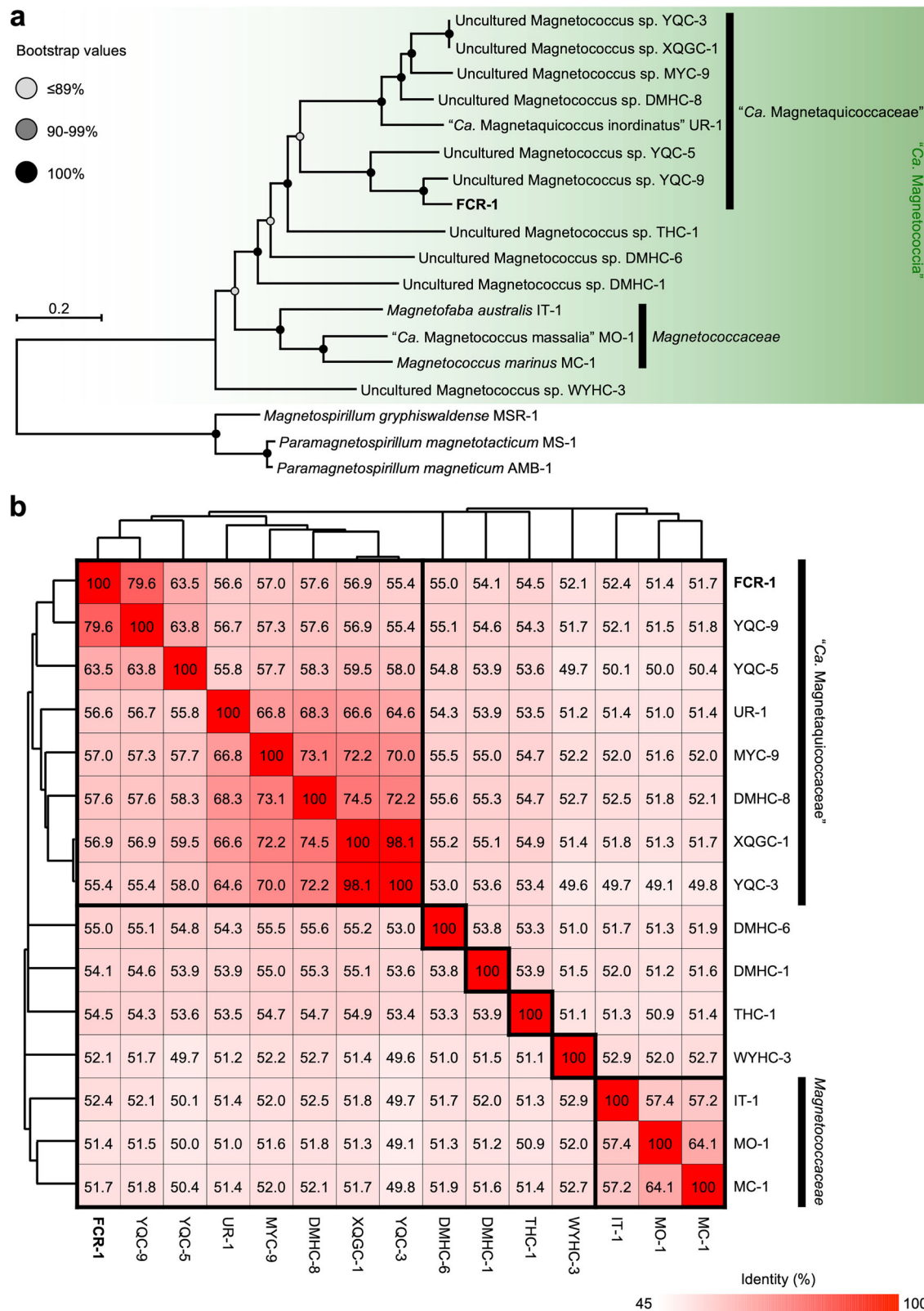


Fig. 5 | Phylogenomic tree based on ubiquitous single-copy marker genes and whole-genome relationships between strains of the class "*Ca. Magnetococcia*".
a ML tree based on 36 concatenated single-copy marker genes showing the position of strain FCR-1 and 14 well-characterized uncultured and cultured strains of magnetotactic "*Ca. Magnetococcia*". The marker genes of magnetotactic

Alphaproteobacteria, *Paramagnetospirillum magnetotacticum* MS-1, *Paramagnetospirillum magneticum* AMB-1 and *Magnetospirillum gryphiswaldense* MSR-1, are used as the outgroup. The scale bar represents amino acid substitutions per site. **b** Heat maps showing pairwise comparisons of the AAI between the "*Ca. Magnetococcia*" strains. The thermal colour scale is shown at the bottom right.

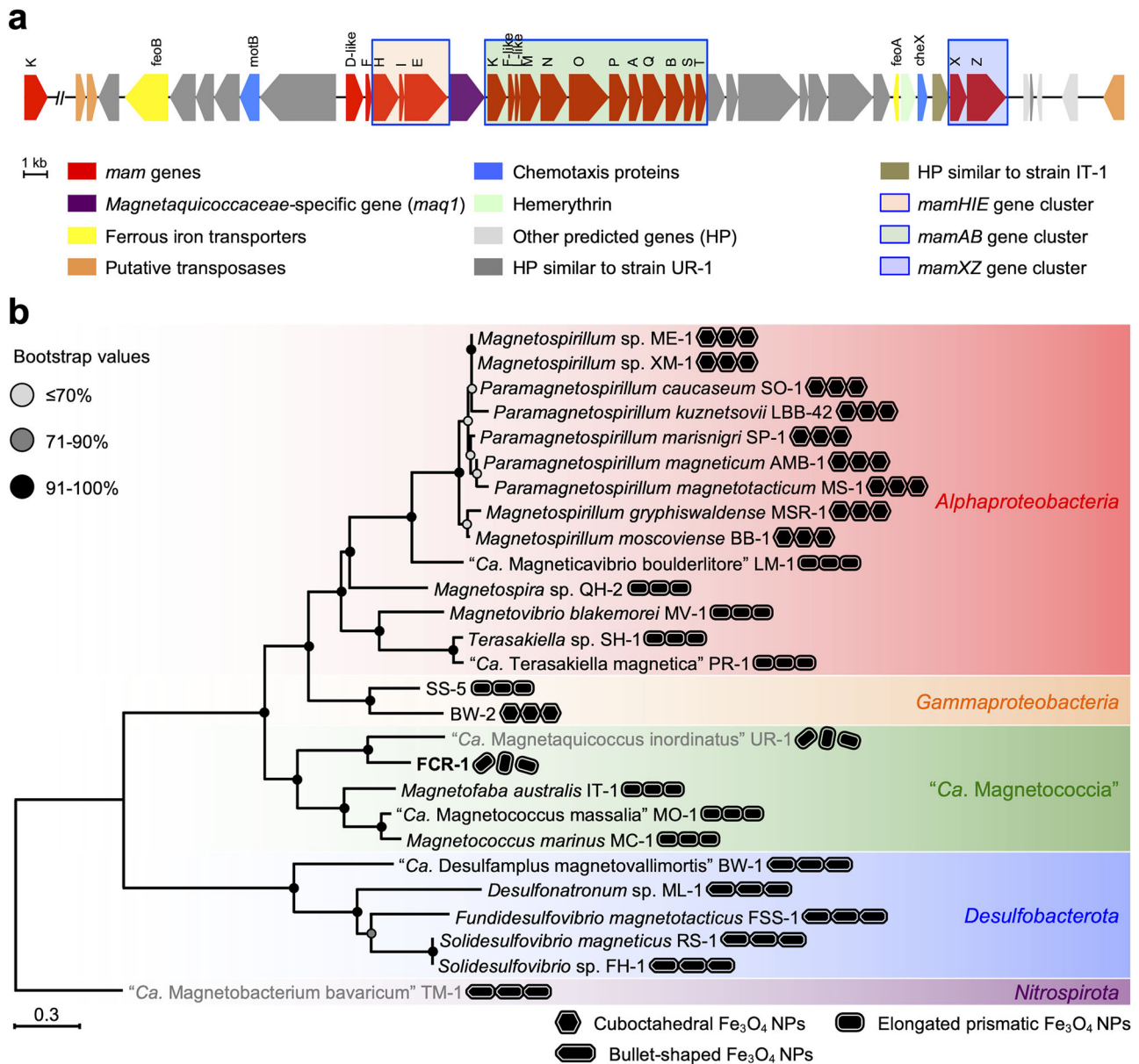


Fig. 6 | Magnetosome gene cluster and the phylogenetic tree based on magnetosome proteins. a Organization of a gene cluster containing putative magnetosome- and magnetotaxis-associated genes. **b** ML tree based on the concatenated eight core magnetosome proteins (MamABEIKMPQ) showing the position of strain FCR-1 and 24 well-characterized cultured strains of magnetotactic "Ca. Magnetococcia", Alphaproteobacteria, Gammaproteobacteria and Desulfobacterota

except for uncultured "Ca. Mq. inordinatus" UR-1. The magnetosome proteins of magnetotactic Nitrospirata, uncultured "Ca. Magnetobacterium bavaricum" TM-1, are used as the outgroup. Cultured and uncultured MTB are shown in black and dark grey, respectively. The scale bar represents amino acid substitutions per site.

SIID45300_02189) and one gene encoding putative transposase (locus_tag: SIID45300_02232) were found in the upstream and downstream of the region, respectively. All of the putative magnetosome- and magnetotaxis-associated genes were found in the contig 4 (2,294,037 bp). The MGC contained 42 genes, 20 genes of which showed a high degree of similarity with the *mam* genes of the strains of magnetotactic "Ca. Magnetococcia" and Alphaproteobacteria (Fig. 6a and Supplementary Data). The second *mamK* gene (locus_tag: SIID45300_01378) was found in approximately 1012 kb upstream of the gene encoding putative transposase (locus_tag: SIID45300_02188). The *mamAB* gene cluster contained the *mamK*, *mamF*-like, *mamL*-like, *mamM*, *mamN*, *mamO*, *mamP*, *mamA*, *mamQ*, *mamB*, *mamS* and *mamT* genes (Fig. 6a). The *mamHIE* gene cluster was found in the upstream of the *mamAB* gene cluster, and the *mamD*-like and *mamF* genes were located in the

upstream of the *mamHIE* gene cluster. The *mamXZ* gene cluster was also found in the downstream of the *mamAB* gene cluster. The *Magnetaquicoccaceae*-specific gene (*maq1*) was located between the *mamHIE* and *mamAB* gene clusters in FCR-1 genome as in the case of "Ca. Mq. inordinatus" UR-1¹⁹. A *feoB* gene was located in the upstream of the *mamHIE* gene cluster, which was similar to that of *Mf. australis* IT-1. A *feoA* gene was also located in the upstream of the *mamXZ* gene cluster, similar to that found in *Terasakiella* sp. SH-1. The gene encoding chemotaxis protein MotB was found in the upstream of the *mamD*-like gene, while the gene encoding chemotaxis protein CheX was located between the *mamAB* and *mamXZ* gene clusters. The gene encoding hemerythrin was located between the *feoA* gene and the *cheX* gene. This region also contained 18 hypothetical proteins (HPs); 14 genes with a high degree of similarity to the genes encoding HP in the putative MGC of "Ca. Mq.

inordinatus" UR-1, 1 gene with the putative MGC of *Mf. australis* IT-1, but 3 genes not found in any known MTB.

Phylogenetic analysis based on the concatenated amino acid sequences of eight core magnetosome proteins (MamABEIKMPQ) showed that strain FCR-1 formed a separate clade with uncultured "*Ca. Mq. inordinatus*" UR-1 biomineralizing unchained elongated prismatic Fe_3O_4 NPs and located away from three cultured strains of the family *Magnetococcaceae* biomineralizing chained elongated prismatic Fe_3O_4 NPs (Fig. 6b). To investigate the diverse magnetosome chain configuration in the class "*Ca. Magnetococcia*", the phylogenetic analysis was also performed by using MamK protein sequences of well-characterized uncultured and cultured strains of the class "*Ca. Magnetococcia*" containing single-copy or multicopy *mamK* genes. Intriguingly, the phylogenetic tree based on MamK proteins showed that the second *mamK* gene outside the MGC of strain FCR-1 was located away from the *mamK* gene inside the MGC, while the "*Ca. Magnetococcia*" strains biomineralizing a single chain of magnetosome formed a separate clade (Supplementary Fig. 12 in the Supplementary Information). Furthermore, the sequence similarity between the *mamK* genes and the morphology of Fe_3O_4 NPs might be correlated with magnetosome chain configuration in the "*Ca. Magnetococcia*" strains containing multicopy *mamK* genes (Supplementary Fig. 13 in the Supplementary Information). The similarity between the MamK proteins and the shape factor of strain FCR-1 showed 47% and 0.65, which were consistent with the protein sequence similarity ($\leq 66\%$) and the shape factor (≤ 0.69). Comparative analysis of the MGC of strain FCR-1 with that of the "*Ca. Magnetococcia*" strains showed that strain FCR-1, YQC-9 and UR-1, which biomineralize unchained magnetosomes, possessed *maq1* gene (Supplementary Fig. 14 and Supplementary Table 1 in the Supplementary Information).

Discussion

Freshwater magnetotactic cocci were discovered more than 40 years ago and frequently found from various freshwater habitats¹³. However, the freshwater magnetotactic cocci remain uncultivated before this work. We have reported in the above the isolation of a novel freshwater magnetotactic coccus FCR-1 that biomineralizes unchained magnetosomes. Axenic culture of the freshwater magnetotactic coccus FCR-1 was successfully attained, verified by the genomic sequencing, and we found that almost all of the FCR-1 cells biomineralized unchained magnetosomes unlike commonly observed chained magnetosomes (Supplementary Fig. 5 in the Supplementary Information). Strain FCR-1 also had the ability to form Poly P granules containing either magnesium or calcium in individual cells (Fig. 3f, g, Supplementary Figs. 6, 7 in the Supplementary Information, and Supplementary Data). However, it still remains unknown why strain FCR-1 mainly biomineralized unchained magnetosomes and formed Poly P granules containing magnesium or calcium. We found that strain FCR-1 belongs to the family "*Ca. Magnetaquicoccaceae*" within the class "*Ca. Magnetococcia*" and represents a novel genus of the family "*Ca. Magnetaquicoccaceae*" (Figs. 2, 5 and Supplementary Fig. 11 in the Supplementary Information). Interestingly, the 16S rRNA gene sequence of strain FCR-1 was the same as the sequence of uncultured magnetotactic coccus clone HCH0515, which was detected from freshwater sediments of moat, Xi'an city, China²⁸. On the basis of the above result and the fact that Chichijima has never been connected to the Eurasia continent, it can be inferred that strain FCR-1 might have migrated by carriers such as migratory birds and/or yellow sand.

In the present study, we, for the first time, isolated and cultivated strain FCR-1 in a semi-solid medium, in which an oxygen concentration gradient was established, using gellan gum as a gelling agent. Note that gellan gum is an extracellular polysaccharide produced by *Sphingomonas elodea* and usually used as a gelling agent for plant tissue culture and cultivation of thermophilic microorganisms that grow at high temperature. In fact, some of the previous studies suggested that gellan gum could be used as a gelling agent for cultivation and isolation of mesophilic microorganisms from soil and freshwater environments^{31,32}. Strain FCR-1 grew in a semi-solid medium, in which an oxygen concentration gradient was established, using

Bacto agar as a gelling agent, but the growth rate was lower than that grown in the semi-solid gellan gum medium, whereas strain FCR-1 was unable to grow in an oxygen-gradient semi-solid medium using Noble agar as a gelling agent. Although agar is commonly used in microbiological studies, it could be a potential inhibitor of the growth of some of microorganisms^{33,34}. It is therefore supposed that agar slowed the growth of FCR-1 cells. Thanks to gellan gum, which forms highly transparent gels, a very fine band of cells was easily observed by the naked eye. Therefore, semi-solid gellan gum media can be a useful tool for observation of the process of forming a band of cells, and isolation and cultivation of as-yet-uncultured MTB, including uncultured microaerophilic MTB, which form a very fine band of cells.

In contrast to *Mc. marinus* MC-1¹⁵ and *Mf. australis* IT-1¹⁷, strain FCR-1 was unable to oxidize thiosulphate when grown chemolithoautotrophically (Table 1 and Supplementary Fig. 3 in the Supplementary Information). The essential *sox* genes for oxidizing thiosulphate such as *soxXYZAB* operon and putative *sox* genes are present in the *Mc. marinus* MC-1 genome¹⁵. As in the case of several strains of the class "*Ca. Magnetococcia*"²⁰, strain FCR-1 contained the *soxY* (locus_tag: SIID45300_02975) and *soxZ* (locus_tag: SIID45300_02974) genes, while the *soxA*, *soxB* and *soxX* genes were not found in the genome of strain FCR-1. The absence of several essential *sox* genes is congruent with the experimental result; that is strain FCR-1 was not capable of oxidizing thiosulphate for growth. In addition, strain FCR-1 had the ability to oxidize sulphide, but the strain was not capable of reducing sulphate (Supplementary Fig. 3 in the Supplementary Information). Strain FCR-1 contained *dsrABL* (locus_tag: SIID45300_00713, SIID45300_00712, SIID45300_00711) genes, *dsrMK* (locus_tag: SIID45300_00870, SIID45300_00869) genes and *dsrJOP* (locus_tag: SIID45300_01599, SIID45300_01598, SIID45300_01597) genes, which indicates that the strain is potentially capable of reducing sulphate and oxidizing sulphide and/or sulphur. "*Ca. Mq. inordinatus*" UR-1 also contained *dsrABL* genes, *dsrC* gene and *dsrFEHJOP* genes and the presence of the *dsrEFH* genes and *dsrL* gene indicated the reverse type of Dsr pathway¹⁹. Strain FCR-1 also had the ability to synthesize intracellular elemental sulphur (Supplementary Fig. 8 in the Supplementary Information) and contained *fccA* gene (locus_tag: SIID45300_02979) and *fccB* gene (locus_tag: SIID45300_02980), which are related to oxidation of sulphide to elemental sulphur.

Formation of Poly P granules is commonly found among MTB. Strain FCR-1 formed 1 to 3 Poly P granules containing either magnesium or calcium (Fig. 3f, g, Supplementary Figs. 6, 7 in the Supplementary Information, and Supplementary Data). MTB also often produce intracellular calcium granules such as calcium carbonate (CaCO_3), calcium phosphate and calcium-rich phosphate^{35,36}. Previous studies have shown that calcium phosphate and calcium-rich phosphate can be distinguished by the Ca K α /P K α ratio, in such a way that the former has higher Ca K α /P K α ratio (1.2–2.2) than the latter (0.22–0.26)^{37,38}. The Ca K α /P K α ratio of the Poly P granules in FCR-1 cells showed 0.28 ± 0.02 (Fig. 3f, g and Supplementary Data). Thus, strain FCR-1 produced calcium-rich phosphate granules. Recently, there are reports that freshwater magnetotactic cocci accumulated large Poly P granules under anoxic conditions and hydrolysed the Poly P granules under suboxic conditions, which indicates that the cocci utilized the Poly P for supporting their phosphorus metabolisms^{20,21}. Polyphosphate kinase (PPK) is a main enzyme that catalyses the initial step in the formation of long-chain Poly P using ATP (PPK1) or GTP (PPK2)^{39,40}, while exopolyphosphatase (PPX) has hydrolysis activity that releases the terminal phosphate from Poly P⁴¹. Two genes encoding PPK2 (locus_tag: SIID45300_00168) and exopolyphosphatase/guanosine pentaphosphate phosphohydrolase (PPX/GppA) (locus_tag: SIID45300_01972) were found in the FCR-1 genome. A possible explanation is that the formation or hydrolysis of Poly P granules in FCR-1 cells may require either magnesium or calcium ions for the PPK2 or the PPX/GppA activity. These also indicate that strain FCR-1 significantly contribute to the biogeochemical cycling of iron, sulphur, phosphorus, magnesium and calcium in freshwater environments.

The morphology of magnetosome is correlated with MTB phylogenetic affiliations⁴². The morphology of magnetosomes of strain FCR-1 was

clearly different from that of magnetosomes of three cultured strains of *Mc. marinus* MC-1¹⁵, “*Ca. Mc. massalia*” MO-1¹⁶ and *Mf. australis* IT-1¹⁷ (Table 1). The morphology and spatial arrangement of magnetosome are known to be strictly controlled by the magnetosome-associated genes and therefore it is supposed that the organization of unchained magnetosomes in strain FCR-1 can be determined by the MGC identified in this study. It has been demonstrated that the *mamK*, *mamJ*, *mamY*, *mcaA* and *mcaB* genes, which are involved in the formation of chained magnetosomes, were found only in the genomes of *Magnetospirillum* species^{43–46}. However, as in the case of other strains of the class “*Ca. Magnetococcia*”, the *mamJ*, *mamY*, *mcaA* and *mcaB* genes were not found in the MGC of strain FCR-1, which indicates that some other mechanisms for forming chained magnetosomes are present in this group of MTB^{19,26}. The *mamK* gene, which encodes an actin-like protein and organizes chained magnetosomes⁴³, was found in the MGC of strain FCR-1, noting that the *mamK* gene is commonly present in MTB except for magnetotactic *Elusimicrobiota*¹². As in the case of the “*Ca. Magnetococcia*” strains containing multicopy *mamK* genes^{19,26}, strain FCR-1 also possessed two copies of *mamK* genes located inside and outside of the MGC, which indicates that two MamK proteins are related to the specific spatial arrangement of magnetosomes; that is unchained magnetosomes, in the cell. The copy number of *mamK* genes and the similarity of multicopy *mamK* genes appeared to be associated with diverse magnetosome chain configuration, which indicated that the *mamK* genes of “*Ca. Magnetococcia*” strains biomineralizing unchained magnetosomes had a relatively low similarity with each other ($\leq 67\%$)²⁶. In addition, the relationship between the similarity of the *mamK* genes and the shape factor of magnetosomes illustrated that the elongated shape of Fe_3O_4 NPs might be also correlated with the unchained magnetosomes (Supplementary Fig. 13 in the Supplementary Information). Additionally, the MGC of strain FCR-1 contained several proteins with unknown functions, which may be attributed to the formation of unchained truncated hexagonal prism-like Fe_3O_4 NPs. The *Magnetaquicoccaceae*-specific gene (*maq1*), which is also found in the MGC of strain FCR-1, is located between *mamE* and *mamK* genes in strains belonging to the family “*Ca. Magnetaquicoccaceae*” and similar to the position of *mamJ* gene in the genus *Magnetospirillum*¹⁹, which indicates that the organization of unchained magnetosomes could be attributed to the *maq1* gene. Strain FCR-1, YQC-9 and UR-1, which belong to the family “*Ca. Magnetaquicoccaceae*” and biomineralize unchained magnetosomes, possessed *maq1* gene (Supplementary Fig. 14 and Supplementary Table 1 in the Supplementary Information). However, strain DMHC-6 and THC-1, which biomineralize unchained magnetosomes, did not possess the *maq1* gene, which implies that the biomineralization of unchained magnetosomes is not solely attributed to the *maq1* gene. Three hypothetical proteins (locus_tag: SIID45300_02215, SIID45300_02219, SIID45300_02220) of strain FCR-1 had a homology with those of “*Ca. Mq. inordinatus*” UR-1, but had no homology with any of the proteins of cultured organisms in the GeneBank database. Therefore, these three proteins might be specifically encoded by the members of the family “*Ca. Magnetaquicoccaceae*”, which biomineralize unchained truncated hexagonal prism-like Fe_3O_4 NPs (Fig. 6a and Supplementary Data). In future work, it would be interesting to create mutants without these three genes in order to elucidate the roles of these proteins. It is of great interest and importance to understand the mechanism of the biomineralization of unchained magnetosomes from both ecological and evolutionary points of view. From a thermodynamical point of view, the configuration of magnetosomes should be determined based on the free energy minimal conditions; i.e., the energy is lowered by the formation of chains, whereas the entropy is increased in the case of unchained (disassembled) magnetosomes. In other words, both configurations of magnetosomes; that is, chained or unchained ones, are possible as long as the free energy is minimal. However, the total magnetization of each magnetotactic bacterium containing chained magnetosomes is higher than that containing unchained magnetosomes. Therefore, it is advantageous for MTB to possess chained magnetosomes in terms of efficient migrations along geomagnetic field lines, which may explain why most of MTB form chained magnetosomes.

Detailed characteristics that distinguish strain FCR-1 from *Mf. australis* IT-1, “*Ca. Mc. massalia*” MO-1 and *Mc. marinus* MC-1 are summarized in Table 1. In conclusion, strain FCR-1 is a novel freshwater magnetotactic coccus belonging to the family “*Ca. Magnetaquicoccaceae*” that biomineralizes unchained truncated hexagonal prismatic Fe_3O_4 NPs. We tentatively name strain FCR-1 “*Candidatus Magnetaquiglobus chichijimensis*”.

Description of novel candidate genus and species

***Candidatus Magnetaquiglobus*.** *Magnetaquiglobus* (Mag.net.a.qui.glo'bus. L. n. *magnês -etis* a magnet; N.L. pref. *magneto-*, pertaining to a magnet; L. fem. n. *aqua* water; N.L. masc. n. *globus*, a sphere; N.L. masc. n. *Magnetaquiglobus* the magnetic sphere from water, referring to its sphere morphology and magnetotactic behaviour).

***Candidatus Magnetaquiglobus chichijimensis*.** *Magnetaquiglobus chichijimensis* (chi.chi.jim.en'sis L. gen. n. *chichijimensis*, pertaining to Chichijima Island, referring to the source of the sediment sample from which the strain was isolated).

Methods

Sample collection, physicochemical analysis and distribution of MTB

Sediment located around 0.2 m under the surface of freshwater of Renju Dam in Chichijima, Tokyo, Japan (27.071084°N, 142.206201°E) was collected together with freshwater in May 2021 under the official permission by the Ogasawara Village Office, and transferred to two 2-litre plastic bottles (Fig. 1a). The plastic bottles were incubated in the laboratory at room temperature (approximately 24 °C) in dim light for 5 months for the creation of a microcosm (Fig. 1b). The pH, salinity and chemical oxygen demand (COD) of the water in the microcosm were, respectively, measured with a pH/ion metre (LAQUA F-72, Horiba, Japan), digital refractometer (PAL-06S, Atago, Japan) and water quality pack test (Kyoritsu Chemical-check Laboratory, Japan). To investigate the vertical distributions of chemical species in the water and sediment in the microcosm, the concentrations of dissolved oxygen (DO) and chemical species (F^- , Br^- , Cl^- , NO_3^- , NO_2^- , NH_4^+ , SO_4^{2-} , PO_4^{3-}) were measured by a dissolved oxygen metre (Seven2Go Pro, Mettler Toledo, Switzerland) and ion chromatograph (ICS-2100, DIONEX, USA). The concentration of DO was measured from approximately 8.0 cm above the surface of sediment down to approximately 4.0 cm deep at 0.5 or 1.0 cm intervals. The water above the sediment and pore water in the sediment were sucked out by sterile needle-syringes at 1.0 cm intervals from −4.0 cm to 8.0 cm, where the water-sediment interface is located at 0 cm. The water and pore water samples were centrifuged and sterilely filtered for measuring the profiles of the chemical species. The number of MTB at each spot was also counted by an optical microscope (DM5000B, Leica, Germany) using the hanging-drop method.

16S rRNA gene amplicon sequencing

Amplicon sequencing of 16S rRNA gene was carried out by Techno Suruga Laboratory Co. Ltd. (Shizuoka, Japan). Genomic DNA was extracted from magnetically enriched MTB cells with an MORA-EXTRACT kit (Kyokuto Pharmaceutical, Japan). Amplicon sequencing for the V3-V4 region of the 16S rRNA gene was conducted with an MiSeq system (Illumina, USA) and MiSeq Reagent Kit v3 (600 cycles) (Illumina, USA), following the manufacturer's instruction. The obtained pair-end (2× 300 bp) reads were dimultiplexed with Usearch6.1.544_i86⁴⁷, merged with fastq-join software⁴⁸, trimmed to remove the primer sequences with Cutadapt version 1.18 software⁴⁹ and filtered with FASTX-Toolkit software to guarantee the quality of the products⁵⁰. Operational taxonomic units (OTUs) (similarity threshold: 97%) were generated by QIIME1.8.0 software⁵¹ and assessed using the Greengenes Database version 13.8⁵². The raw 16S rRNA gene amplicon sequencing data were deposited in the DDBJ/EMBL/GenBank database under the following accession number: DRR586105.

Isolation and culture conditions of freshwater magnetotactic coccus FCR-1

The MTB cells were collected by neodymium-iron-boron magnets ($\phi 10 \times 10$ mm) of 480 mT, attaching them to the outer surface of the bottles at approximately 1 cm above the sediment-water interface for 60 min, and then the cells accumulated by the magnets were collected with a Pasteur pipette. The MTB cells were then magnetically enriched by an MTB trap device for 30 min²⁷. For the cultivation and isolation of a freshwater magnetotactic coccus, we developed a new semi-solid gellan gum medium named “Freshwater magnetotactic cocci medium”, abbreviated to “FMC medium”, which was composed of 0.5 mg L⁻¹ of resazurin, 0.01 g L⁻¹ of NaNO₃, 0.02 g L⁻¹ of NH₄Cl, 0.05 g L⁻¹ of MgCl₂•6H₂O, 0.03 g L⁻¹ of CaCl₂•2H₂O, 0.05 g L⁻¹ of casamino acids (Becton, Dickinson and Company, USA), 5.0 mL L⁻¹ of modified Wolfe’s mineral elixir^{53,54} and 3.0 g L⁻¹ of gellan gum (Fujifilm-Wako, Japan). The modified Wolfe’s mineral elixir contained the following salts (per litre of distilled water): 1.50 g nitrotri-acetic acid, 2.48 g MgCl₂•6H₂O, 0.42 g MnCl₂•4H₂O, 1.0 g NaCl, 0.097 g FeCl₃•6H₂O, 0.15 g CoCl₂•6H₂O, 0.30 g CaCl₂•2H₂O, 0.086 g ZnCl₂, 0.014 g CuCl₂•2H₂O, 0.02 g KAl(SO₄)₂•12H₂O, 0.01 g H₃BO₃, 0.4 g Na₂MoO₄•2H₂O, 0.035 g NiCl₂•6H₂O and 0.3 mg Na₂SeO₃•5H₂O, and the pH of the mineral solution was adjusted to 7.0. Glass culture tubes with screw caps and butyl rubber stoppers were filled with the medium up to approximately 4/5 (26 mL) of their volume (32 mL) and autoclaved. After having been autoclaved, the medium was kept at 50 °C, sparged with 100% N₂ gas (0.3 L min⁻¹) for 5 min, and then the following solutions were added to the medium (per litre of distilled water): 5.0 mL of a sterile anaerobic stock of vitamin solution¹⁴, 2.8 mL of a sterile anaerobic stock of 0.25 M potassium phosphate buffer (pH 7.0), 4.0 mL of a sterile anaerobic stock of 100 mM sodium acetate, 10.0 mL of a sterile anaerobic stock of 5% sodium bicarbonate and 4.0 mL of 5% (w/v) freshly made neutralized and filter-sterilized cysteine•HCl•H₂O (pH 7.0). The final pH of the FMC medium was 7.4–7.8. The medium was placed without shaking at room temperature and the colour of resazurin reagent changed from pink to colourless after 1 day. To establish a gradient in the oxygen concentration, 6.0 mL of filter-sterilized air (approximately 3.9% O₂) was added to the headspace of the screw-capped glass culture tubes 1 h before inoculation.

Magnetotactic cocci enriched by the MTB trap device were inoculated in the OATZ in the FMC medium. The magnetotactic cocci were cultivated in the medium at room temperature in dim light until a band of cells were observed in the OATZ. An axenic culture of cells was then obtained by the MTB trap device²⁷, followed by dilution-to-extinction. After three-time purifications by dilution-to-extinction technique, the state of the axenic culture was evaluated by optical and electron microscopy and sequencing of the 16S rRNA gene.

The optimal growth conditions were determined in duplicate experiments, changing the amount of air, temperature, pH, and ferrous chloride and gellan gum concentrations as follows; (a) 0, 1.0, 2.0, 3.0, 4.0, 5.0 and 6.0 mL of filter-sterilized air was introduced into the headspace (6.0 mL) of the screw-capped glass culture tubes, (b) the temperature range; 15, 20, 24, 28, 32 and 37 °C, (c) 10 mM MOPS buffer was added to the medium in the case of pH 6.6 and 7.0, (d) 10 mM HEPES buffer was added to the medium in the case of pH 7.0, 7.4, 7.8 and 8.2, (e) 10 mM Bicine buffer was added to the medium in the case of pH 8.2 and 8.6, (f) the FeCl₂•4H₂O concentrations; 0, 6, 12 and 25 µM and (g) the gellan gum concentrations; 0, 1.5, 3.0, 6.0 and 12.0 g L⁻¹. In addition, the FCR-1 cells were grown in the semi-solid medium using 1.5 or 3.0 g L⁻¹ of Bacto agar (Becton, Dickinson and Company, USA), and 1.5 or 3.0 g L⁻¹ of Noble agar (Becton, Dickinson and Company, USA) as gelling agents instead of gellan gum. To test for the possibility of the heterotrophic growth, the following carbon/energy sources were added to the casamino acids- and sodium acetate-free FMC medium; that is, sodium formate, sodium acetate, disodium succinate, disodium fumarate, sodium pyruvate, sodium citrate, sodium malate, sodium tartrate and sodium lactate, the final concentration of which was 0.4 mM. In order to examine the ability of the FCR-1 cells to grow chemolithoautotrophically, they were grown in the casamino acids- and sodium acetate-free semi-solid gellan gum

medium containing 0.5 g L⁻¹ of sodium bicarbonate as a major carbon source and 0.05, 0.1 or 0.2 g L⁻¹ of Na₂S₂O₃•5H₂O, 0.05, 0.1 or 0.2 g L⁻¹ of Na₂S•9H₂O and 0.05, 0.1 or 0.2 g L⁻¹ of Na₂SO₃ as an electron donor. Additionally, the FCR-1 cells were grown under anaerobic conditions using the casamino acids- and sodium acetate-free FMC liquid medium containing 0.4 mM sodium lactate as an electron donor and 0.05, 0.1 or 0.2 g L⁻¹ of Na₂SO₄, and 0.05, 0.1 or 0.2 g L⁻¹ of Na₂SO₃ as an electron acceptor in order to investigate the capability of dissimilatory sulphate reduction. When growth was observed, the growth cultures were transferred three times into fresh media containing the same electron donor or carbon source.

The optimal medium for strain FCR-1 among the examined conditions mentioned above was the FMC medium supplemented with 10 mM HEPES buffer (pH 7.8). 0.5 g L⁻¹ of freshly made and filter-sterilized 5% sodium bicarbonate solution was added to the medium just before sparging the medium with 100% N₂ gas (0.3 L min⁻¹) for 5 min. 1.0 mL of filter-sterilized air (approximately 0.8% O₂) was added to the headspace of the screw-capped glass culture tubes 1 h before inoculation. The FCR-1 cells were grown routinely in the modified FMC medium at room temperature in dim light for 14 days. The motility (magnetotaxis) was checked by an optical microscope (DM5000B, Leica, Germany) in a magnetic field generated by a ferrite magnet (20 × 5 × 30 mm, 80 mT; Niroku Seisakusho, Japan) using the hanging drop method.

To conduct whole genome sequencing analysis, we specially designed a liquid medium excluding gellan gum, which was composed of 0.5 mg L⁻¹ of resazurin, 0.3 g L⁻¹ of NaNO₃, 0.05 g L⁻¹ of MgCl₂•6H₂O, 0.03 g L⁻¹ of CaCl₂•2H₂O, 0.6 g L⁻¹ of casamino acids (Becton, Dickinson and Company, USA), 0.1 g L⁻¹ of sodium acetate and 5.0 mL L⁻¹ of the modified Wolfe’s mineral elixir^{53,54}. Glass culture vials with aluminium caps and butyl rubber stoppers were filled with the medium up to approximately 2/3 (45 mL) of their volume (68 mL) and autoclaved. After having been autoclaved and cooled down to room temperature, 1.0 g L⁻¹ of freshly made and filter-sterilized sodium bicarbonate solution was added to the medium and bubbled with 100% N₂ gas (0.3 L min⁻¹) for 5 min, and then the following solutions were added to the medium (per litre of distilled water); 10.0 mL of a sterile anaerobic stock of 1 M HEPES buffer (pH 7.8), 5.0 mL of a sterile anaerobic stock of vitamin solution¹⁴, 2.8 mL of a sterile anaerobic stock of 0.25 M potassium phosphate buffer (pH 7.0), 4.0 mL of 5% (w/v) freshly made neutralized and filter-sterilized cysteine•HCl•H₂O (pH 7.0) and 2.5 mL of a sterile anaerobic stock of 10 mM FeCl₂•4H₂O. The liquid medium was placed statically for 1 day and reduced by cysteine and ferrous chloride. 2.0 mL of filter-sterilized air (approximately 0.6% O₂) was added to the headspace of the glass culture vials. After 1 h, the formation of an oxygen concentration gradient was confirmed by the colour change of the surface of the medium from transparent to pink while the bottom remained transparent. The FCR-1 cells were gently inoculated at the pink-colourless interface near the surface of the medium and statically cultivated at room temperature in dim light for 14 days without disturbing the oxygen concentration gradient. When the medium changed from pink to colourless due to the consumption of oxygen by growing cells, 1.0 mL of filter-sterilized air (approximately 0.3% O₂) was added to the headspace of the glass culture vials for increasing the cell concentrations. The final cell concentration reached $(1.0 \pm 0.5) \times 10^6$ cells/mL. The FCR-1 cells were grown in a total volume of 990 mL (45 mL × 22) of the liquid medium for genome sequencing analysis.

Phylogenetic analysis of 16S rRNA gene sequence

The full-length 16S rRNA gene sequencing was carried out by Techno Suruga Laboratory Co. Ltd. (Shizuoka, Japan). The genomic DNA was extracted from the culture of FCR-1 cells using Cica Geneus DNA Extraction Reagent ST (Kanto Chemical, Japan) and the 16S rRNA gene was amplified using the universal bacterial primers 27F (5'-AGAGTTTG ATCCTGGCTCAG-3') and 1492R (5'-GGTACCTTGTTCAGACTT-3') as previously described⁵⁵. The PCR product was directly sequenced using the ABI PRISM 3500xL Genetic Analyzer System (Applied Biosystems, USA) with a BigDye Terminator version 3.1 Cycle Sequencing Kit (Applied

Biosystems, USA) following the manufacturer's instruction. The obtained sequences were assembled and analysed with ChromasPro 2.1 (Technelysium, Australia). The 16S rRNA gene sequence (1423 bp) was deposited in the DDBJ/EMBL/GenBank database under the following accession number: LC781547. The sequence similarity search was performed using the NCBI BLAST tools (<http://www.ncbi.nlm.nih.gov/BLAST>)⁵⁶. The nucleotide sequence alignment of 16S rRNA gene sequences from strain FCR-1 and some other related strains of the class “*Ca. Magnetococcia*” was performed using the MUSCLE algorithm of MEGA11 version 11.0.13 software^{57,58}. The maximum-likelihood (ML) tree was constructed with the MEGA11 using the GTR + G + I model⁵⁹ with 1000 bootstrap replicates and complete deletion options.

Transmission electron microscopy (TEM)

FCR-1 cells were placed on a TEM grid (200 mesh Cu Formvar/carbon-coated grid, JEOL, Japan) and air-dried at room temperature. The grid was rinsed three times with sterile distilled water and then the cells were observed by a TEM (JEM-2100, JEOL, Japan) at an accelerating voltage of 160 kV. The number of magnetic NPs in each cell was counted targeting at 100 individual cells. The sizes of cells and magnetic NPs were measured based on 100 cells and 506 magnetic NPs, respectively, from several TEM micrographs using Digital Micrograph software (Gatan, USA). Energy dispersive X-ray spectroscopy (EDS) analysis was performed by a TEM (JEM-2200FS, JEOL, Japan) at an accelerating voltage of 200 kV. EDS elemental mapping was conducted on the annular dark-field-scanning TEM (ADF-STEM) mode with a JED-2300T EDS spectrometer (JEOL, Japan). STEM-EDS data analyses were performed with the Analysis Station software (JEOL, Japan). High-resolution (HR) TEM and electron energy loss spectroscopy (EELS) analyses were conducted by a TEM (JEM-ARM200F) with a Schottky gun (JEOL, Japan) equipped with a probe aberration corrector at an acceleration voltage of 200 kV. EELS data were obtained using a dispersion of 0.25 eV per channel to record the spectra in the energy loss ranging from 690 to 750 eV with an energy resolution of approximately 1.2 eV, which was determined by the full width at half maximum of the zero-loss peak. The dwell time was optimized to obtain sufficient signal intensity. Magnetite (Fe₃O₄) NPs (average size of 25 nm, Sigma-Aldrich, USA) and hematite (α-Fe₂O₃) powder (average size of 0.3 μm, Koujundo Chemical Laboratory, Japan) were used as the reference iron oxide samples for EELS analysis. The hematite powders were pounded in a mortar to obtain finer particles. We also obtained fast Fourier transform (FFT) patterns using Digital Micrograph software (Gatan, USA).

Genome sequencing and phylogenomic analysis

For whole genome sequencing, FCR-1 cells were collected by centrifugation and washed three times with 5 mM EDTA-10 mM HEPES buffer (pH7.0). The whole genome sequencing was carried out by Techno Suruga Laboratory Co. Ltd. (Shizuoka, Japan). Genomic DNA was extracted from strain FCR-1 using a Genomic-tip 20/G (QIAGEN, Germany) and assessed by the 5200 Fragment Analyzer System (Agilent Technologies, USA) using an Agilent HS Genomic DNA 50 kb kit (Agilent Technologies, USA). The DNA was purified with DNA Clean Beads (MGI Tech Co., Ltd., China). A SMRTbell library was constructed with a SMRTbell Express Template Prep kit 2.0 (Pacific Biosciences, USA) and sequenced using the PacBio Revio system (Pacific Biosciences, USA) following the manufacturer's instruction. High-fidelity (HiFi) long-reads were obtained by using SMART link software version 13.0.207600. The Ultra-Low PCR adapters, PCR duplicate reads and short reads (≤1000 bp) were removed with lima version 2.7.1⁶⁰, pbmarkdup version 1.0.3 and Filtlong version 0.2.1 (<https://github.com/rrwick/Filtlong>), respectively. The draft genome sequence was constructed using Flye version 2.9.2-b1786 with default settings⁶¹ and the completeness and contamination rates were assessed by CheckM2 version 1.0.1⁶². Annotation of the FCR-1 genome was mainly performed using Prokka version 1.14.6⁶³. The taxonomic assignment of strain FCR-1 was obtained by GTDB-Tk version 2.4.0⁶⁴. The draft genome sequence was deposited in the

DDBJ/EMBL/GenBank database under the following accession number: BAAFGK010000000.

The available genome sequences of strain FCR-1 and 17 strains of magnetotactic “*Ca. Magnetococcia*” and *Alphaproteobacteria* (Fig. 5a and Supplementary Data) were used for a hidden Markov model (HMM) search against 120 single-copy marker genes generated by the GTDB-Tk⁶⁴. 36 universal single-copy marker genes were obtained from the HMM search and the concatenated alignments of the marker genes were aligned with MAFFT version 7.511⁶⁵. An ML tree was constructed with IQ-Tree version 2.1.3 using the LG + F + I + R4 model with 1000 ultrarapid bootstrap replicates. The final consensus tree produced by the IQ-Tree was visualized with FigTree version 1.4.3. The average nucleotide identity (ANI) and average amino acid identity (AAI) were calculated using the ANI/AAI-Matrix online service⁶⁶. Digital DNA-DNA hybridization (dDDH) values were determined using the Genome-to-Genome Distance Calculator (GGDC) 2.1 online software⁶⁷. The available genome sequences from strain FCR-1 and 14 strains of magnetotactic “*Ca. Magnetococcia*” (Fig. 5b and Supplementary Data) were used for phylogenomic analyses.

Analyses of magnetosome- and magnetotaxis-associated genes

The putative magnetosome gene cluster (MGC) of the strain FCR-1 genome was verified with BLAST searches in comparison with the reference MTB sequences and with KEGG Automatic Annotation Server (KAAS)⁶⁸. Homologous amino acid sequences of magnetosome proteins were identified using BLASTP of NCBI (*E*-value < 1e−05). The amino acid sequence alignments of MamA, -B, -E, -I, -K, -M, -P and -Q from strain FCR-1 and 26 strains of magnetotactic “*Ca. Magnetococcia*”, *Alphaproteobacteria*, *Gammaproteobacteria*, *Desulfobacterota* and *Nitrospirota* (Fig. 6b and Supplementary Data) including *Solidesulfobivrio* sp. FH-1 (accession number: AGG16197-AGG16218) and *Desulfonatronum* sp. ML-1 (accession number: AFZ77009-AFZ88982) were performed using the MAFFT version 7.511⁶⁵. The ML tree was constructed with IQ-Tree version 2.1.3 using the LG + F + R5 model with 1,000 ultrarapid bootstrap replicates. The final consensus tree produced by the IQ-Tree was visualized with FigTree version 1.4.3.

Statistics and reproducibility

We investigated the distribution of MTB and chemical species in a microcosm from a single experiment. All of the growth tests of strain FCR-1 were carried out more than or equal to twice up to five times to ensure reproducibility. The size of FCR-1 cells was measured based on 100 cells. The swimming speed of FCR-1 cells was measured based on 343 cells. The number of magnetosomes per cell was counted targeting at 100 cells. The number of FCR-1 cells containing unchained magnetosomes was measured based on 100 cells. The diameter of a flagellum was measured based on 277 flagella. The number of Poly P granules including magnesium or calcium was measured based on 100 cells. The EELS analyses of magnetic NPs contained in five cells were carried out, targeting at more than seven Fe₃O₄ NPs in each cell. The size of magnetic NPs was measured based on 506 Fe₃O₄ NPs.

Reporting summary

Further information on research design is available in the Nature Portfolio Reporting Summary linked to this article.

Data availability

The amplicon sequencing data of the 16S rRNA genes of MTB magnetically enriched from a microcosm were deposited in the DDBJ under the accession number DRR586105. The GenBank/EMBL/DDBJ accession number of the 16S rRNA gene sequence of strain FCR-1 is LC781547. The GenBank/EMBL/DDBJ accession number of the draft genome sequence of strain FCR-1 is BAAFGK010000000. The numerical source data for the graphs and table are provided in the “Supplementary Data”. All the other data are available from the corresponding author on reasonable request.

Received: 11 November 2024; Accepted: 21 March 2025;
Published online: 27 March 2025

References

- Ishizuka, O et al. Early stages in the evolution of Izu-Bonin arc volcanism: New age, chemical, and isotopic constraints. *Earth. Planet. Sci. Lett.* **250**, 385–401 (2006).
- Losos, JB & Ricklefs, RE Adaptation and diversification on islands. *Nature* **457**, 830–836 (2009).
- Kobayashi, S A list of the vascular plants occurring in the Ogasawara (Bonin) Islands. *Ogasawara. Res* **1**, 1–33 (1978).
- Ohbayashi, T, Inaba, M, Suzuki, H & Kato, M List of insects in the Ogasawara Islands, Japan (2002). *Ogasawara. Res.* **29**, 17–74 (2004).
- Karube, H, Matsumoto, K, Kishimoto, T & Ozono, A Records of notable insect species from the Ogasawara Islands. *Ogasawara. Res.* **38**, 1–15 (2012).
- Bazylinski, DA & Frankel, RB Magnetosome formation in prokaryotes. *Nat. Rev. Microbiol.* **2**, 217–230 (2004).
- Uebe, R & Schüller, D Magnetosome biogenesis in magnetotactic bacteria. *Nat. Rev. Microbiol.* **14**, 621–637 (2016).
- Lefèvre, CT & Bazylinski, DA Ecology, diversity, and evolution of magnetotactic bacteria. *Mol. Biol. Rev.* **77**, 497–526 (2013).
- Lin, W et al. Genomic expansion of magnetotactic bacteria reveals an early common origin of magnetotaxis with lineage-specific evolution. *ISME J.* **12**, 1508–1519 (2018).
- Lin, W et al. Expanding magnetic organelle biogenesis in the domain Bacteria. *Microbiome* **8**, 152 (2020).
- Uzun, M, Koziaeva, V, Dziuba, M, Leão, P, Krutkina, M & Grouzdev, D Detection of interphylum transfers of the magnetosome gene cluster in magnetotactic bacteria. *Front. Microbiol.* **13**, 945734 (2022).
- Uzun, M et al. Recovery and genome reconstruction of novel magnetotactic *Elusimicrobiota* from bog soil. *ISME J.* **17**, 204–214 (2023).
- Liu, P et al. Diverse phylogeny and morphology of magnetite biomineralized by magnetotactic cocci. *Environ. Microbiol.* **23**, 1115–1129 (2021).
- Frankel, RB, Bazylinski, DA, Johnson, MS & Taylor, BL Magneto-aerotaxis in marine coccoid bacteria. *Biophys. J.* **73**, 994–1000 (1997).
- Bazylinski, DA et al. *Magnetococcus marinus* gen. nov., sp. nov., a marine, magnetotactic bacterium that represents a novel lineage (*Magnetococcaceae* fam. nov., *Magnetococcales* ord. nov.) at the base of the *Alphaproteobacteria*. *Int. J. Syst. Evol. Microbiol.* **63**, 801–808 (2013).
- Lefèvre, CT, Bernadac, A, Yu-Zhang, K, Pradel, N & Wu, LF Isolation and characterization of a magnetotactic bacterial culture from the Mediterranean Sea. *Environ. Microbiol.* **11**, 1646–1657 (2009).
- Morillo, V et al. Isolation, cultivation and genomic analysis of magnetosome biomineralization genes of a new genus of South-seeking magnetotactic cocci within the *Alphaproteobacteria*. *Front. Microbiol.* **5**, 72 (2014).
- Lefèvre, CT et al. Diversity of magneto-aerotactic behaviors and oxygen sensing mechanisms in cultured magnetotactic bacteria. *Biophys. J.* **107**, 527–538 (2014).
- Koziaeva, V, Dziuba, M, Le-ao, P, Uzun, M, Krutkina, M & Grouzdev, D Genome-based metabolic reconstruction of a novel uncultivated freshwater magnetotactic coccus “Ca. Magnetaquicoccus inordinatus” UR-1, and proposal of a candidate family “Ca. Magnetaquicoccaceae”. *Front. Microbiol.* **10**, 2290 (2019).
- Rivas-Lamelo, S et al. Magnetotactic bacteria as a new model for P sequestration in the ferruginous Lake Pavin. *Geochem. Perspect. Lett.* **5**, 35–41 (2017).
- Schulz-Vogt, HN et al. Effect of large magnetotactic bacteria with polyphosphate inclusions on the phosphate profile of the suboxic zone in the Black Sea. *ISME J.* **13**, 1198–1208 (2019).
- Bidaud, CC et al. Biogeochemical niche of magnetotactic cocci capable of sequestering large polyphosphate inclusions in the anoxic layer of the Lake Pavin water column. *Front. Microbiol.* **12**, 789134 (2022).
- Cox, BL et al. Organization and elemental analysis of P-, S-, and Fe-rich inclusions in a population of freshwater magnetococci. *Geomicrobiol. J.* **19**, 387–406 (2002).
- Araujo, ACV et al. Combined genomic and structural analyses of a cultured magnetotactic bacterium reveals its niche adaptation to a dynamic environment. *BMC Genomics* **17**, 726 (2016).
- Li, J, Menguy, N, Leroy, E, Roberts, AP, Liu, P & Pan, Y Biomineralization and magnetism of uncultured magnetotactic coccus strain with non-chained magnetosomal magnetite nanoparticles. *J. Geophys. Res. Solid. Earth.* **125**, e2020JB020853 (2020).
- Liu, P et al. Key gene networks that control magnetosome biomineralization in magnetoactive bacteria. *Natl. Sci. Rev.* **10**, nwac238 (2023).
- Jogler, C et al. Toward cloning of the magnetotactic metagenome: identification of magnetosome island gene clusters in uncultivated magnetotactic bacteria from different aquatic sediments. *Appl. Environ. Microbiol.* **75**, 3972–3979 (2009).
- Wang, Y, Lin, W, Li, J & Pan, Y High diversity of magnetotactic *Deltaproteobacteria* in a freshwater niche. *Appl. Environ. Microbiol.* **79**, 2813–2817 (2013).
- Goris, J, Konstantidis, KT, Klappenbach, JA, Coenye, T, Vandamme, P & Tiedje, JM DNA–DNA hybridization values and their relationship to whole-genome sequence similarities. *Int. J. Syst. Evol. Microbiol.* **57**, 81–91 (2007).
- Auch, AF, von Jan, M, Klenk, HP & Göker, M Digital DNA–DNA hybridization for microbial species delineation by means of genome-to-genome sequence comparison. *Stand. Genom. Sci.* **2**, 117–134 (2010).
- Janssen, PH, Yates, PS, Grinton, BE, Taylor, PM & Sait, M Improved culturability of soil bacteria and isolation in pure culture of novel members of the divisions *Acidobacteria*, *Actinobacteria*, *Proteobacteria*, and *Verrucomicrobia*. *Appl. Environ. Microbiol.* **68**, 2391–2396 (2002).
- Tamaki, H, Hanada, S, Sekiguchi, Y, Tanaka, Y & Kamagata, Y Effect of gelling agent on colony formation in solid cultivation of microbial community in lake sediment. *Environ. Microbiol.* **11**, 1827–1834 (2009).
- Tanaka, T et al. A hidden pitfall in the preparation of agar media undermines microorganism cultivability. *Appl. Environ. Microbiol.* **80**, 7659–7666 (2014).
- Klein, T, Poghosyan, L, Barclay, JE, Murrell, JC, Hutchings, MI & Lehtovirta-Morley, LE Cultivation of ammonia-oxidising archaea on solid medium. *FEMS Microbiol. Lett.* **369**, fnac029 (2022).
- Taoka, A, Kondo, J, Oestreicher, Z & Fukumori, Y Characterization of uncultured giant rod-shaped magnetotactic *Gammaproteobacteria* from a fresh water pond in Kanazawa, Japan. *Microbiology* **160**, 2226–2234 (2014).
- Liu, P et al. A novel magnetotactic *Alphaproteobacterium* producing intracellular magnetite and calcium-bearing minerals. *Appl. Environ. Microbiol.* **87**, e01556–21 (2021).
- Cosmidis, J, Benzerara, K, Nassif, N, Tylliszczak, T & Bourdelle, F Characterization of Ca-phosphate biological materials by scanning transmission X-ray microscopy (STXM) at the Ca L₂, 3-, P L₂, 3-, and C K-edges. *Acta Biomater.* **12**, 260–269 (2015).
- Li, JH et al. Biomineralization patterns of intracellular carbonatogenesis in cyanobacteria: molecular hypothesis. *Minerals* **6**, 10 (2016).
- Ahn, K & Kornberg, A Polyphosphate kinase from *Escherichia coli*. Purification and demonstration of a phosphoenzyme intermediate. *J. Biol. Chem.* **265**, 11734–11739 (1990).

40. Rao, NN, Gómez-García, MR & Kornberg, A Inorganic polyphosphate: essential for growth and survival. *Annu. Rev. Biochem.* **78**, 605–647 (2009).
41. Akiyama, M, Crooke, E & Kornberg, A An exopolyphosphatase of *E. coli*: the enzyme and its ppx gene in a polyphosphate operon. *J. Biol. Chem.* **268**, 633–639 (1993).
42. Pósai, M, Lefèvre, CT, Trubitsyn, D, Bazylnski, DA & Frankel, RB Phylogenetic significance of composition and crystal morphology of magnetosome minerals. *Front. Microbiol.* **4**, 344 (2013).
43. Scheffel, A, Gruska, M, Faivre, D, Linaoudis, A, Plitzko, JM & Schüler, D An acidic protein aligns magnetosomes along a filamentous structure in magnetotactic bacteria. *Nature* **440**, 110–114 (2006).
44. Abreu, N, Mannoubi, S, Ozyamak, E, Pignol, D, Ginot, N & Komeili, A Interplay between two bacterial actin homologs, MamK and MamK-Like, is required for the alignment of magnetosome organelles in *Magnetospirillum magneticum* AMB-1. *J. Bacteriol.* **196**, 3111–3121 (2014).
45. Toro-Nahuelpan, M et al. MamY is a membrane-bound protein that aligns magnetosomes and the motility axis of helical magnetotactic bacteria. *Nat. Microbiol.* **4**, 1978–1989 (2019).
46. Wan, J et al. McaA and McaB control the dynamic positioning of a bacterial magnetic organelle. *Nat. Commun.* **13**, 5652 (2022).
47. Edgar, RC, Haas, BJ, Clemente, JC, Quince, C & Knight, R UCHIME improves sensitivity and speed of chimera detection. *Bioinformatics* **27**, 2194–2200 (2011).
48. Aronesty, E Comparison of sequencing utility programs. *Open. Bioinforma. J.* **7**, 1–8 (2013).
49. Martin, M Cutadapt removes adapter sequences from high-throughput sequencing reads. *EMBnet. J.* **17**, 10–12 (2011).
50. Gordon, A. & Hannon, G. J. FASTX-Toolkit FASTQ/A short-reads preprocessing tools [software]. Available from: http://hannonlab.cshl.edu/fastx_toolkit/index.html (2012).
51. Caporaso, JG et al. QIIME allows analysis of high-throughput community sequencing data. *Nat. Methods* **7**, 335336 (2010).
52. DeSantis, TZ et al. Greengenes, a chimera-checked 16S rRNA gene database and workbench compatible with ARB. *Appl. Environ. Microbiol.* **72**, 5069–5072 (2006).
53. Wolin, EA, Wolin, MJ & Wolfe, RS Formation of methane by bacterial extracts. *J. Biol. Chem.* **238**, 2882–2886 (1963).
54. Bazylnski, DA, Dean, AJ, Schüler, D, Phillips, EJ & Lovley, DR N₂-dependent growth and nitrogenase activity in metal-metabolizing bacteria, *Geobacter* and *Magnetospirillum* species. *Environ. Microbiol.* **2**, 266–273 (2000).
55. Lane, D. J. 16S/23S rRNA sequencing. In: *Nucleic acid techniques in bacterial systematics* (eds, Stackebrandt, E. & Goodfellow, M.) 115–175 (John Wiley and Sons, 1991).
56. Altschul, SF et al. Gapped BLAST and PSI-BLAST: a new generation of protein database search programs. *Nucleic Acids Res.* **25**, 3389–3402 (1997).
57. Edgar, RC MUSCLE: multiple sequence alignment with high accuracy and high throughput. *Nucleic Acids Res.* **32**, 1792–1797 (2004).
58. Tamura, K, Stecher, G & Kumar, S MEGA 11: molecular evolutionary genetics analysis version 11. *Mol. Biol. Evol.* **38**, 3022–3027 (2021).
59. Nei, M. & Kumar, S. *Molecular Evolution and Phylogenetics* (Oxford University Press, New York, 2000).
60. Topfer, A. Lima - The PacBio Barcode Demultiplexer (2018). Available at: <https://github.com/PacificBiosciences/barcoding> (accessed January 25, 2018).
61. Kolmogorov, M, Yuan, J, Lin, Y & Pevzner, P Assembly of long error-prone reads using repeat graphs. *Nat. Biotechnol.* **37**, 540–546 (2019).
62. Chklovski, A, Parks, DH, Woodcroft, BJ & Tyson, GW CheckM2: a rapid, scalable and accurate tool for assessing microbial genome quality using machine learning. *Nat. Methods* **20**, 1203–1212 (2023).
63. Seemann, T Prokka: rapid prokaryotic genome annotation. *Bioinformatics* **30**, 2068–2069 (2014).
64. Parks, DH et al. A standardized bacterial taxonomy based on genome phylogeny substantially revises the tree of life. *Nat. Biotechnol.* **36**, 996–1004 (2018).
65. Katoh, K, Rozewicki, J & Yamada, KD MAFFT online service: multiple sequence alignment, interactive sequence choice and visualization. *Brief. Bioinform* **20**, 1160–1166 (2019).
66. Rodriguez-R, L & Konstantinidis, K The enveomics collection: a toolbox for specialized analyses of microbial genomes and metagenomes. *PeerJ. Prepr.* **4**, e1900v1 (2016).
67. Meier-Kolthoff, JP, Auch, AF, Klenk, HP & Göker, M Genome sequence-based species delimitation with confidence intervals and improved distance functions. *BMC Bioinforma.* **14**, 60 (2013).
68. Moriya, Y, Itoh, M, Okuda, S, Yoshizawa, AC & Kanehisa, M KAAAS: an automatic genome annotation and pathway reconstruction server. *Nucleic Acids Res.* **35**, 182–185 (2007).

Acknowledgements

The present study was carried out as part of the “Bio-Nano Innovation Programme: Development of advanced functional nano materials and devices, and their application to biotechnology” organized by the Bio-Nano Electronics Research Centre, Toyo University. We would like to thank Toyo University for raising a fund for the above programme since April 2021. We would like to thank Dr. Ken Takai, Japan Agency for Marine-Earth Science and Technology, for the use of an ion chromatograph and a micro dissolved oxygen sensor. We would like to thank Dr. Takashi Itoh, Japan Collection of Microorganisms, RIKEN BioResource Research Center, for his advice on the storage of strain FCR-1. We would like to thank the Ogasawara Village Office for their official permission to collect the sediment samples from Renju Dam.

Author contributions

H.Sm. organized the present research project, and designed and performed experiments. H.Sm. and K.Y. performed TEM observations and data analyses. M.M. performed ion chromatographic measurements. Y.T. and S.S. performed bioinformatics data processing. H.Sm. and Y.T. performed phylogenetic and genomic analyses. H.N. performed DO concentration measurements. H.Sm. and A.T. performed identification of a putative MGC. M.F., H.Sr. and A.T. performed cultivation and data analyses. H.K. collected samples. H.Sm. and T.M. wrote the manuscript. T.M. raised the fund. All of the authors checked the manuscript including figures and tables and agreed with the contents of the paper.

Competing interests

The authors declare no competing interests.

Additional information

Supplementary information The online version contains supplementary material available at <https://doi.org/10.1038/s42003-025-07981-5>.

Correspondence and requests for materials should be addressed to Hirokazu Shimoshige.

Peer review information *Communications Biology* thanks Wei Lin and the other, anonymous, reviewer for their contribution to the peer review of this work. Primary Handling Editor: Tobias Goris. A peer review file is available.

Reprints and permissions information is available at <http://www.nature.com/reprints>

Publisher's note Springer Nature remains neutral with regard to jurisdictional claims in published maps and institutional affiliations.

Open Access This article is licensed under a Creative Commons Attribution-NonCommercial-NoDerivatives 4.0 International License, which permits any non-commercial use, sharing, distribution and reproduction in any medium or format, as long as you give appropriate credit to the original author(s) and the source, provide a link to the Creative Commons licence, and indicate if you modified the licensed material. You do not have permission under this licence to share adapted material derived from this article or parts of it. The images or other third party material in this article are included in the article's Creative Commons licence, unless indicated otherwise in a credit line to the material. If material is not included in the article's Creative Commons licence and your intended use is not permitted by statutory regulation or exceeds the permitted use, you will need to obtain permission directly from the copyright holder. To view a copy of this licence, visit <http://creativecommons.org/licenses/by-nc-nd/4.0/>.

© The Author(s) 2025